Drought acclimation of Quercus ilex leaves improves tolerance to moderate drought but not resistance to severe water stress

Jean-Marc Limousin, Amélie Roussel, Jesús Rodríguez-Calcerrada, José M Torres-Ruiz, Myriam Moreno, Laura Garcia de Jalon, Jean-Marc Ourcival, Guillaume Simioni, Hervé Cochard, Nicolas Martin-StPaul

Drought acclimation of *Quercus ilex* leaves improves tolerance to moderate drought but not resistance to severe water stress

Jean-Marc Limousin[1]*, Amélie Roussel[1], Jesús Rodríguez-Calcerrada[2], José M. Torres-Ruiz[3], Myriam Moreno[4], Laura Garcia de Jalon[1], Jean-Marc Ourcival[1], Guillaume Simioni[4], Hervé Cochard[3], Nicolas Martin-StPaul[4]

[1] CEFE, Univ Montpellier, CNRS, EPHE, IRD, 1919 Route de Mende, 34293 Montpellier Cedex 5, France

[2] Departamento de Sistemas y Recursos Naturales, ETSI Montes, Forestal y del Medio Natural, Universidad Politécnica de Madrid Ciudad Universitaria s/n, 28040, Madrid, Spain

[3] University Clermont-Auvergne, INRA, PIAF, 63000 Clermont-Ferrand, France

[4] Unité Ecologie des Forêts Méditerranéennes (UR629), INRA, Domaine Saint Paul, Site Agroparc, 84914 Avignon cedex 9, France

* Corresponding author: Jean-Marc Limousin, jean-marc.limousin@cefe.cnrs.fr

Abstract

Increasing temperature and drought can result in leaf dehydration and defoliation even in drought-adapted tree species such as the Mediterranean evergreen *Quercus ilex* L. The stomatal regulation of leaf water potential plays a central role in avoiding this phenomenon and is constrained by a suite of leaf traits including hydraulic conductance and vulnerability, hydraulic capacitance, minimum conductance to water vapor, osmotic potential and cell wall elasticity. We investigated whether the plasticity in these traits may improve leaf tolerance to drought in two long-term rainfall exclusion experiments in Mediterranean forests. Osmotic adjustment was observed to lower the water potential at turgor loss in the rainfall-exclusion treatments, thus suggesting a stomatal closure at more negative water potentials and a more anisohydric behavior in drier conditions. Conversely, leaf hydraulic conductance and vulnerability did not exhibit any plasticity between treatments so the hydraulic safety margins were narrower in the rainfall-exclusion treatments. The sequence of leaf responses to seasonal drought and dehydration was conserved among treatments and sites but trees were more likely to suffer losses of turgor and hydraulic functioning in the rainfall-exclusion treatments. We conclude that leaf plasticity might help the trees to tolerate moderate drought but not to resist severe water stress.

Keywords

Evergreen broadleaf, Hydraulic vulnerability, Osmotic adjustment, Plasticity, Rainfall exclusion, Safety margin, Stomatal regulation, Turgor loss, Water potential

Introduction

Climate warming and shifts in rainfall patterns in many regions of the globe, and particularly in the Mediterranean, have led to increasingly frequent and severe drought episodes (IPCC, 2013; Trenberth *et al.* 2014; Tramblay *et al.* 2020) and have triggered widespread tree mortality (Allen *et al.* 2010; Carnicer *et al.* 2011; Senf *et al.* 2020). In the last decade of research in plant ecophysiology, hydraulic failure, which is the loss of xylem hydraulic function due to embolism inhibiting vascular water transport, has been considered the main physiological mechanism involved in drought-induced tree dieback and mortality (McDowell *et al.* 2008; Adams *et al.* 2017; Choat *et al.* 2018). Hydraulic traits are thus central for predicting tree ability to cope with rapid climate change and more severe drought events, and the phenotypic plasticity of these traits is crucial in allowing the trees to acclimate to increasing water limitation (Choat *et al.* 2018).

As xylem embolism develops because of excessive tension in the sap during drought-stress, the hydraulic safety margin, *i.e.* the difference between the minimum xylem water potential experienced by plants in the field and the water potential leading to hydraulic failure, has become a central concept for understanding tree vulnerability to drought (Choat *et al.* 2012; Delzon and Cochard 2014; Anderegg *et al.* 2016; Martin-StPaul *et al.* 2017). This hydraulic safety margin is governed, on one hand, by the xylem vulnerability to tension-induced embolism and, on the other hand, by the dynamic regulation of plant water potential, which mainly involves the leaf ability to balance gas exchange with hydraulic properties (Sperry 2000; Sperry *et al.* 2016). While the large inter-specific variations in xylem resistance to embolism explain most of the differences in hydraulic safety margins among species (Martin-StPaul *et al.* 2017), intra-specific variations for this trait are generally small, and not clearly related to climate (Martinez-Vilalta *et al.* 2009; Lamy *et al.* 2014; Schuldt *et al.* 2016; Torres-Ruiz *et al.* 2019). Moreover, plastic changes of the xylem vulnerability to embolism have not yet been observed in adult trees in response to experimentally increased drought intensity (*e.g.* Limousin *et al.* 2010a; Hudson *et al.* 2018). Conversely, hydraulic acclimation to drought is known to occur through reductions of the leaf area to sapwood area ratio, which, besides limiting tree water use, can limit the drop in plant water potential along the transpiration stream (Mencuccini and Grace 1995; Martinez-Vilalta *et al.* 2009; Martin-StPaul *et al.* 2013). The regulation of leaf water potential by stomata is also under the control of the leaf turgor pressure (Brodribb and Holbrook 2003; Rodriguez-Dominguez *et al.* 2016), which depends on the leaf osmotic potential and the cell wall elasticity, two traits known to plastically respond to drought (Bartlett

et al. 2014; Nolan *et al.* 2017). Therefore, we hypothesize that any adjustment of the hydraulic safety margin in response to drought mostly arises on the side of the leaf water potential regulation.

Leaf hydraulics may play a crucial role in this adjustment for three main reasons. First, because the leaves are the primary siege of plant gas-exchange, the stomata-bearing organs and the most distal part along the soil-plant hydraulic pathway. Leaves are thus the organs experiencing the most negative water potentials and the organs ultimately responsible for water potential regulation in the whole plant. Second, because in accordance with the vulnerability segmentation hypothesis, leaves would be more hydraulically vulnerable than other organs such as branches and stems, (Tyree and Ewers 1991; Zhu *et al.* 2016; Charrier *et al.* 2016; Scoffoni and Sack 2017). Consequently, the leaves are expected to be the first organs to exhibit signs of hydraulic failure during severe water stress, and may thereby act as a 'safety-valve' protecting the rest of the plant from excessively negative water potentials (Tyree *et al.* 1993; Wolfe *et al.* 2016; Scoffoni and Sack 2017). Third, because leaf hydraulic conductance and vulnerability to hydraulic failure involve both xylem and outside-xylem pathways, which may each respond differently to water stress (Cochard *et al.* 2004; Trifilo *et al.* 2016; Scoffoni *et al.* 2017; Scoffoni and Sack 2017). The response to drought of leaf hydraulic functions is thus more difficult to predict than that of branches, but leaves are also more likely to respond plastically and acclimate to drought (Martorell *et al.* 2015).

The leaf tolerance to drought entails a complex sequence of water potential thresholds leading to functional failure because stomatal closure, leaf wilting and loss of hydraulic conductivity all have different sensitivities to water stress (Bartlett *et al.* 2016; Trueba *et al.* 2019). While the coordination between the stomatal regulation of leaf water potential and the xylem vulnerability to hydraulic failure has been long described (Tyree and Sperry 1988, Jones and Sutherland 1991, Salleo *et al.* 2000; Cochard *et al.* 2002), the actual relationship between plant resistance to drought and stomatal behavior appears far more complicated to apprehend (Martinez-Vilalta and Garcia-Forner 2017; Martin-StPaul *et al.* 2017). Difficulties to link the leaf regulation of water potential with plant resistance to drought arise from the complexity of the physiological mechanisms by which stomata sense and regulate leaf water potential (Brodribb *et al.* 2017; Buckley 2019; Creek *et al.* 2020), the large diversity of stomatal regulation strategies that can exist among species (Klein 2014, Martinez-Vilalta *et al.* 2014), the magnitude of the minimum leaf conductance to water vapor that continues after stomatal closure (Duursma *et al.* 2018), and the need to preserve sufficient soil water reserves and plant

water storage in order to survive long drought events (Blackman *et al.* 2016; Martin-StPaul *et al.* 2017). Therefore, the regulation of leaf water potential and hence the leaf tolerance to water stress can hypothetically acclimate to drought in several different ways.

We investigated whether leaf water potential regulation and tolerance to drought can be affected by plastic adjustments in adult trees exposed to a long-term reduction in water availability. Two types of datasets were obtained from two long-term rainfall exclusion experiments set up in forest ecosystems: a multi-year dataset of predawn and midday leaf water potentials measured over a wide range of drought conditions, and a dataset of traits related to leaf hydraulics and water relations measured several years after the start of the experimental rainfall exclusions. We studied the widespread Mediterranean evergreen oak *Quercus ilex* L., a drought adapted sclerophyll species (Salleo and Lo Gullo 1990) characterized by a low xylem vulnerability to embolism (Lobo *et al.* 2018) that has nevertheless exhibited signs of drought-induced dieback in the last decades (Lloret *et al.* 2004; Gentilesca *et al.* 2017; Rodriguez-Calcerrada *et al.* 2017). We characterized the leaf water potential regulation across sites and rainfall treatments, and measured different leaf traits related to leaf gas exchange, turgor and hydration maintenance, and hydraulic functions. We investigated (1) whether the regulation of leaf water potential could change in response to drier climatic conditions, and (2) whether plasticity in leaf traits could change leaf stomatal tolerance and hydraulic resistance to water stress. Our results aim to provide novel information regarding how increased aridity conditions might affect leaf gas exchange, leaf area and drought-induced tree mortality under the expected climate change.

Materials and Methods

Experimental sites

Table 1. Main characteristics of the two experimental sites used in the study

	Puéchabon	Font-Blanche
Location	35 km north-west of Montpellier 43°44'29''N, 3°35'45''E 270 m above sea level	20 km east of Marseille 43°14'27''N, 5°40'45''E 425 m above sea level
Mean annual temperature (2008-2017)	13.8°C	14.0°C
Mean annual precipitation (2008-2017)	965 mm	701 mm
Soil description	silty clay loam 75 % - 90% rock fraction limestone bedrock	silty clay loam 50 % - 90% rock fraction limestone bedrock
Dominant tree species	holm oak (*Quercus ilex* L.)	Aleppo pine (*Pinus halepensis* Mill.) holm oak (*Quercus ilex* L.)
Tree height	5.5 m	pine: 13.5 m oak: 6.5 m
Basal area	27.4 m²/ha	total: 37.3 m²/ha oak: 10.1 m²/ha
Leaf area index (LAI)	2.2	2.9
Rainfall exclusion	PVC gutters hung below canopy -29 % of net precipitation 140 m² plots exclusion since 2003	PVC gutters hung below canopy -29 % of net precipitation 625 m² plots exclusion since 2009
References	Limousin *et al.* (2009)	Moreno *et al.* (2021)

Leaf and branch material were collected in two forests in Southern France where the evergreen *Quercus ilex* L. is the dominant or co-dominant tree species and where partial rainfall exclusion experiments have been carried out for several years: the Puéchabon and Font-Blanche experimental sites. The Puéchabon site is a dense coppice strongly dominated by *Q. ilex* and located 35 km northwest of Montpellier (43°44'29'' N; 3°35'46'' E, 270 m a.s.l.; Limousin *et al.* 2009). The Font-Blanche site is a mixed *Pinus halepensis – Q. ilex* forest located 20 km east of Marseille (43°14'27''N, 5°40'45''E, 425 m a.s.l.; Moreno *et al.* 2021). The two sites are located 177 km away from each other but are remarkably similar regarding their edaphic, climatic and experimental set-up conditions (see Table 1 for a summary of the main characteristics of the sites). Their main difference is the presence of an upper canopy strata of Aleppo pine (*P. halepensis*) in Font-Blanche, which is absent in Puéchabon. The two sites have

been set-up with similar partial rainfall exclusion systems by using PVC gutters hung at a height of 1.5 m to 2 m above ground, so as to cover one third of the plot area and exclude approximately 30% of the net precipitation. In the control plots, similar gutters have been installed upside-down to homogenize albedo and understorey microclimate. The experiments have been continuously operated since March 2003 in Puéchabon and January 2009 in Font-Blanche, so trees had been exposed to 30% rainfall exclusion for 15 and 9 years, respectively, at the time of branch sampling (March 2018).

Field measurements of leaf water potential, stomatal conductance and mesophyll conductance

Predawn and midday leaf water potential (hereafter Ψ_{Pd} and Ψ_{Md}, respectively) were measured regularly at the two sites since the start of the rainfall exclusion experiments. Depending on the site and on the year, measurements were carried out from three to twelve times a year between Spring and Autumn, with the aim of covering the range of water stress experienced by the trees in every particular year. In Puéchabon, data were available for 11 years and 92 dates (from 2003 to 2009, in 2011, and from 2015 to 2017; Bykova *et al.* 2018); and in Font-Blanche, data were available for 9 years and 36 dates (from 2009 to 2017; Moreno *et al.* 2021). Four to six *Q. ilex* trees per treatment were sampled for water potential at each site. In Puéchabon, until 2011, two to three leaves per tree were sampled from a scaffold and immediately measured with a pressure chamber (PMS1000; PMS Instruments, Corvallis, OR, USA). Since 2015, small twigs were sampled, bagged in humid and air-tight plastic bags and stored in a dark cooler for less than 1.5 hours until measured with the PMS chamber. In Font-Blanche, one small twig was sampled from each measured tree, bagged as in Puéchabon and kept in a dark cooler for less than 1.5 hours until measured with a homemade Scholander-type pressure chamber. The comparability of the results between sites was verified by a comparison of the two methods (immediate measurements or bagging) performed during one campaign in Puéchabon in 2016, and an inter-comparison of the pressure chambers in the lab in 2018. Both comparisons yielded non-significant differences (data not shown). The same sampling was repeated at midday for Ψ_{Md} using samples from a well-lit part of the canopy. Using the large number of measurements available for each individual tree (>30 for every tree taking all years together), the relationships between Ψ_{Pd} and Ψ_{Md} were characterized for each individual following Meinzer *et al.* (2016). We calculated the slope of the linear relationship between Ψ_{Md} and Ψ_{Pd}, the minimum Ψ_{Md} when Ψ_{Pd} is equal to zero (Ψ_{Md} @ Ψ_{Pd}=0), the water potential at which predawn and midday

water potentials become equal ($\Psi_{Md} = \Psi_{Pd}$), and the 'hydroscape' which is the area of the triangle bounded by the 1:1 line and the relationship between Ψ_{Md} and Ψ_{Pd} (see Meinzer *et al.* 2016 for details about the variables and the calculation procedure).

A three-day campaign of leaf gas-exchange measurements was also carried out at the Puéchabon site in November 2017, under well-watered conditions after autumn rainfall events, and thus after the end of the severe 2017 summer drought in the two treatments. Measurements were performed on leaves of the current-year cohort from the upper canopy on 6 trees per treatment and three leaves per tree. Two portable photosynthesis systems (Li-6400, Li-Cor Inc., Lincoln, NE, USA) equipped with a LI-6400-40 Leaf Chamber Fluorometer (Li-Cor Inc., Lincoln, NE, USA) were used to measure leaf stomatal conductance (g_s), leaf photosynthesis and the photochemical efficiency of photosystem II (Φ_{PSII}) after acclimating the leaf in the chamber for 20 min (see Limousin *et al.* 2010b for details about the protocol). Ambient CO_2 concentration was regulated at 400 µmol CO_2 mol^{-1} air, the photosynthetic photon flux density (PPFD) was set at a saturating flux of 1500 µmol m^{-2} s^{-1} and the temperature was maintained between 14°C and 21°C (target at 20°C) depending on the hour and day. The leaf mesophyll conductance to CO_2 (g_m) was calculated as in Limousin *et al.* (2010b) by using the variable electron transport rate method proposed by Harley *et al.* (1992), the specific coefficients for holm oak proposed by Niinemets *et al.* (2005) for the relationship between the photosynthetic electron transport rate and the efficiency of the photosystem II, and the temperature correction coefficients proposed by Bernacchi *et al.* (2002).

Pressure-volume curves

Pressure-volume curves (PV curves) were determined on small leafy shoots collected on 6 trees per treatment and experimental site in March 2018. Selected shoots supported only the last cohort of leaves; i.e. leaves produced during the spring 2017 and that had already experienced the 2017 summer drought. Shoots were cut from the upper parts of the tree canopy, sealed in plastic bags and kept in a cooler for transport to the laboratory where they were stored for less than two days in a 5°C cold chamber prior to measurements. Shoot cut ends were then recut under water, and kept in distilled water overnight in a dark cold chamber to allow their progressive rehydration.

PV curves were obtained using the free transpiration bench drying method (Hinckley *et al.* 1980). Shoot water potential (Ψ) and weight (averaged before and after pressurization) were

repeatedly measured 10 to 14 times over the course of the day (typically during 7h to 10h) while the shoot was allowed to dehydrate. Shoot water potential was measured using the PMS pressure chamber (PMS1000; PMS Instruments, Corvallis, OR, USA). The oversaturation of rehydrated samples, the so-called "plateau effect", was corrected by extrapolating the fresh weight at full turgor from the regression of fresh weight against water potential before the turgor loss (Kubiske & Abrams 1990). Curves of -1/Ψ versus leaf water saturation deficit (1-*RWC*) were constructed and used to derive the PV curve parameters following Dreyer *et al.* (1990): the osmotic potential at full turgor (Π_0), the water potential at the turgor loss point (Ψ_{tlp}), the relative water content at the turgor loss point (RWC_{tlp}), and the fraction of apoplastic water (a_f). The mean modulus of elasticity (ε, MPa) was estimated as the slope of the regression between turgor and *RWC* on the initial portion of the PV curve before turgor loss, and multiplied by the fraction of symplastic water (F_{symp}=1-a_f ; Bartlett *et al.* 2012).

Leaf minimum conductance and mass per area

The leaf minimum conductance to water vapor (g_{min}) was measured using the mass loss of the bench-drying shoots during the PV curve measurements. The temperature and relative humidity over the bench were measured every 5 min with an *RH-T* probe (HMP155A, Vaisala, Helsinki, Finland) positioned 10 cm above the samples, and used to calculate the vapor pressure deficit (*VPD*, kPa). The g_{min} was then calculated following Ewers & Oren (2000) by expressing the rate of water mass loss in mmol s^{-1}, and then dividing it by the *VPD* and multiplying by the atmospheric pressure. The rate of water mass loss was calculated only for the linear portion of the drying curve beyond the turgor loss point to account only for the leaf transpiration rate during severe drought conditions inducing complete stomatal closure. The leaf minimum conductance obtained by this method thus represents both the cuticular conductance and the stomatal leakiness of the leaf (Duursma *et al.* 2018).

After PV curve completion, the leaves were removed from the shoot and scanned on a transmission flatbed scanner (Epson Perfection V800, Seiko Epson, Nagano, Japan) to measure the leaf area with the ImageJ software (National Institutes of Health, Bethesda, MD, USA). Leaf area may have been slightly underestimated due to shrinkage in dehydrated leaves, but this effect is limited in species with high LMA values such as *Q. ilex* (Garnier *et al.* 2001) and was neglected in this study. The leaves and the shoot were then oven dried at 60°C for three days and weighted for their dry mass. The average leaf dry mass fraction of the PV curve shoots

was 79.1 % ± 5.2 %, with no significant differences between sites or treatments (P=0.24 for the site difference, P=0.97 for the treatment difference), thus ensuring that PV curve parameters were not biased by an heterogeneity in shoot morphology. The dry mass of the sample was used to calculate the *RWC* of the PV curve shoots and the leaf dry matter content (*LDMC*, mg g^{-1}) calculated as the ratio of dry mass to fresh mass. The one-side leaf area was used to calculate g_{min} per unit leaf area and the leaf mass per area (*LMA*, g m^{-2}) as the leaf dry mass divided by the leaf area.

Leaf hydraulic conductance and vulnerability curve

In March 2018, when soil water content was replenished in either site and treatment, ca. 40 cm-long branches comprising more than 4 growth units were collected from the upper canopy of several trees per treatment in each experimental site, depending on tree accessibility (6 trees in Puéchabon control treatment, 7 trees in Puéchabon rainfall exclusion treatment, 12 trees in Font-Blanche control treatment, and 6 trees in Font-Blanche rainfall exclusion treatment). The leafy branches were immediately sealed in moist and opaque plastic bags with the cut end immersed in water, and kept at 5°C in a cold chamber for 3 to 6 days before measurements. The leaf hydraulic conductance (K_{leaf}) was measured using the rehydration kinetics method whereby leaves are allowed to rehydrate while connected to a flow meter (Brodribb and Cochard 2009; Blackman and Brodribb 2011). Due to the small size of *Q. ilex* leaves and petioles, K_{leaf} was measured on short leafy shoots bearing several leaves. We assumed that the hydraulic resistance in the short water-filled vessels of the twig could be neglected compared to that of leaves, so the leafy-shoot hydraulic conductance expressed per unit leaf area was considered equivalent to the leaf hydraulic conductance (similarly to Brodribb and Cochard 2009; Blackman and Brodribb 2011, and Torres-Ruiz *et al.* 2015). Shoots from the most recent growth unit, i.e. shoots produced in spring 2017 and having experienced the 2017 summer drought, were debarked over approximately 1 cm, wrapped in Parafilm (Sigma-Aldrich Merck, Darmstadt, Germany) where the bark had been removed to prevent leaks, excised under water with a razor blade and immediately connected to a high resolution flowmeter (50 g h^{-1} max flow, Bronkhorst, Ruurlo, Netherland) while maintained in water to prevent transpiration. The flow rate was logged every 0.1 s until it decreased to approximately half of the maximum as shoot rehydrated. The initial Ψ_{leaf} prior to shoot rehydration was measured concomitantly on an adjacent shoot. K_{leaf} was calculated by using the Ohm's law analogy where the pressure gradient across the shoot is equal to - Ψ_{leaf}:

$$K_{leaf} = - I_{max} / (\Psi_{leaf} * LA) \quad (1)$$

K_{leaf} is in mmol s^{-1} MPa^{-1} m^{-2}; I_{max} is the instantaneous maximum flow rate into the shoot (mmol s^{-1}); Ψ_{leaf} is the leaf water potential (MPa) and LA is the leaf area of the shoot (m^2).

Leaf hydraulic vulnerability curves were constructed using the bench drying method by which the large branches were allowed to dehydrate slowly in the lab over the course of one day. The Ψ_{leaf} was checked regularly on small leafy shoots while it was decreasing from a maximum between -0.40 MPa and -0.50 MPa, and several K_{leaf} measurements were performed on different shoots of the same branch at targeted Ψ_{leaf} values. As the number of K_{leaf} measurements that could be performed on one given branch was comprised between 3 and 5 depending on the branch size, the vulnerability curves were constructed by pooling all the measurements from each site and treatment combination. A Weibull function was fitted to the relationship between K_{leaf} and Ψ_{leaf}:

$$K_{leaf} = K_{leaf,max} * \exp(-\Psi_{leaf} / a)^b \quad (2)$$

Where $K_{leaf,max}$ is the maximum leaf hydraulic conductance, and a and b are Weibull parameters used to calculate the K_{leaf} P_{12}, K_{leaf} P_{50}, and K_{leaf} P_{88}, which are, respectively, the Ψ_{leaf} corresponding to a 12% loss, 50% loss or 88% loss of K_{leaf}.

Leaf hydraulic capacitance

The leaf hydraulic capacitance was measured using two independent and complementary methods: one based on the PV curves for measuring the bulk leaf capacitance (C_{bulk}) and the other one based on the rehydration kinetics (while they were connected to the flowmeter) for measuring the leaf capacitance of the leaf tissues directly exchanging water with the transpiration stream (C_{dyn}, Blackman and Brodribb 2011).

C_{bulk} was measured for each individual from the slope of the relationship between leaf RWC and Ψ ($\Delta RWC/\Delta\Psi$), normalized by the leaf area and water content at saturation (Brodribb and Holbrook 2003):

$$C_{bulk} = \Delta RWC/\Delta\Psi * W_{sat}/M * LMA * 1000 \quad (3)$$

where C_{bulk} is in mmol m^{-2} MPa^{-1}, W_{sat} is the saturated mass of water per unit dry mass (g g^{-1}), M is the molar mass of water (g mol^{-1}), and LMA is the leaf dry mass per area (g m^{-2}). C_{bulk} was obtained from the initial part of the PV curve before the turgor loss point. The bulk leaf capacitance was also measured after the turgor loss ($C_{bulk,,tlp}$), when it is no longer influenced by the elasticity of cell walls.

C_{dyn} was calculated by assuming that the rehydration kinetics of leaves is equivalent to the charging of a capacitor through a resistor (Brodribb and Holbrook 2003). The high frequency of flowrate measurements during leaf rehydration were fitted with an analogy of the electric law:

$$I(t) = I_{max} * \exp(-t / \tau) \quad (4)$$

where $I(t)$ is the instantaneous flow rate at any given time, I_{max} is the maximum flow rate as used in Eq. (1), t is the time in second since the moment when I_{max} had been reached, and τ is the time constant of the circuit in second. The time constant τ is equal to the resistance ($= 1/K_{leaf}$) multiplied by the capacitance, so C_{dyn} could be calculated for each rehydrated shoot as:

$$C_{dyn} = \tau * K_{leaf} \quad (5)$$

Statistical analyses

For all the traits measured at the individual tree level, differences among experimental sites and treatments were tested with a two-way ANOVA. The normality distribution of data was verified with the Shapiro test and the homoscedasticity with the Bartlett test, and data were log-transformed to meet these criteria when needed. Weibull hydraulic vulnerability curves were fitted for each site and treatment with the *nls* function in R, and the 95% confidence intervals for their estimates of $K_{leaf}\,P_{12}$, $K_{leaf}\,P_{50}$, and $K_{leaf}\,P_{88}$ were obtained by bootstrapping with the '*fitplc*' R package (Duursma and Choat, 2017). Correlations among traits measured on each individual tree (n=26 trees for traits measured in the laboratory on PV curve samples, and n=17 trees for 'hydroscape' traits or n=12 trees for gas-exchange traits measured in the field) were tested with Pearson's correlation coefficients and a Principal Component Analysis (PCA) after pooling all sites and treatments to increase the statistical power. All the analyses were performed using the R software (version 3.4.3, R Core Team 2017).

Results

Leaf water potential in the field

The two forest sites experience a typical Mediterranean climate with warm and dry summers and a large inter-annual variation in summer precipitation (Fig. 1; Fig. S1). The minimum Ψ_{Pd} experienced annually by the trees in control conditions was observed to correlate positively with summer precipitation in Puéchabon (R^2=0.49, P=0.017) and negatively with summer temperature in Font-Blanche (R^2=0.62, P=0.012). The rainfall exclusion experiments resulted in more negative Ψ_{Pd} values at the peak of drought in the two experimental sites (Fig. 1; Fig. S1). In Puéchabon, treatment differences in annual minimum Ψ_{Pd} were significant in 9 years over 11, and in the last three years before leaf sampling. In Font-Blanche, treatment differences in annual minimum Ψ_{Pd} were significant in 4 years over 9, and in 2 years over the last 3 before leaf sampling. In 2017, the year when the sampled leaves were produced, the climate in spring and summer was remarkably similar between the two sites (Fig. 1c; Table S1). In spite of a wetter spring than in Font-Blanche, Puéchabon experienced significantly lower Ψ_{Pd} in 2017, with values as low as -5.03 MPa and -5.89 MPa in the control and rainfall exclusion treatments, respectively. Font-Blanche experienced the most severe water stress in 2016, with annual minimum Ψ_{Pd} values reaching -3.96 MPa and -4.37 MPa in the control and rainfall exclusion treatments, respectively.

The trajectories of Ψ_{Md} with soil drying and decreasing Ψ_{Pd} differed slightly among sites and rainfall exclusion treatments (Fig. S2; Table 2). Differences were mainly observed between sites, with a smaller 'hydroscape' area, a steeper slope of the relationship between Ψ_{Md} and Ψ_{Pd} and a less negative Ψ_{Md} when Ψ_{Pd}=0, in Font-Blanche than in Puéchabon. These site differences might be due to a lower VPD experienced by the *Q. ilex* trees in Font-Blanche where they grow in the shade of an upper canopy of pines. Conversely, the radiation and VPD experienced by the sunlit leaves in the upper canopy can be considered equivalent between treatments within each site, because reductions of transpiration imposed by the rainfall exclusion probably have a negligible impact on atmospheric VPD in such small scale experimental plots. Therefore, treatment differences in hydroscape were likely influenced by stomatal regulation and leaf hydraulic traits rather than by micro-climatic effects. Trees in the rainfall exclusion treatments had significantly steeper slopes of the regressions between Ψ_{Md} and Ψ_{Pd} (Table 2). The 'hydroscape' areas, the Ψ at which $\Psi_{Md} = \Psi_{Pd}$, and the minimum Ψ_{Md} when Ψ_{Pd}=0 remained

statistically similar between treatments, but there was a tendency for more negative Ψ at which $\Psi_{Md} = \Psi_{Pd}$ and less negative Ψ_{Md} when Ψ_{Pd}=0 in the rainfall exclusion treatments. No interaction between site and the response to rainfall exclusion was detected.

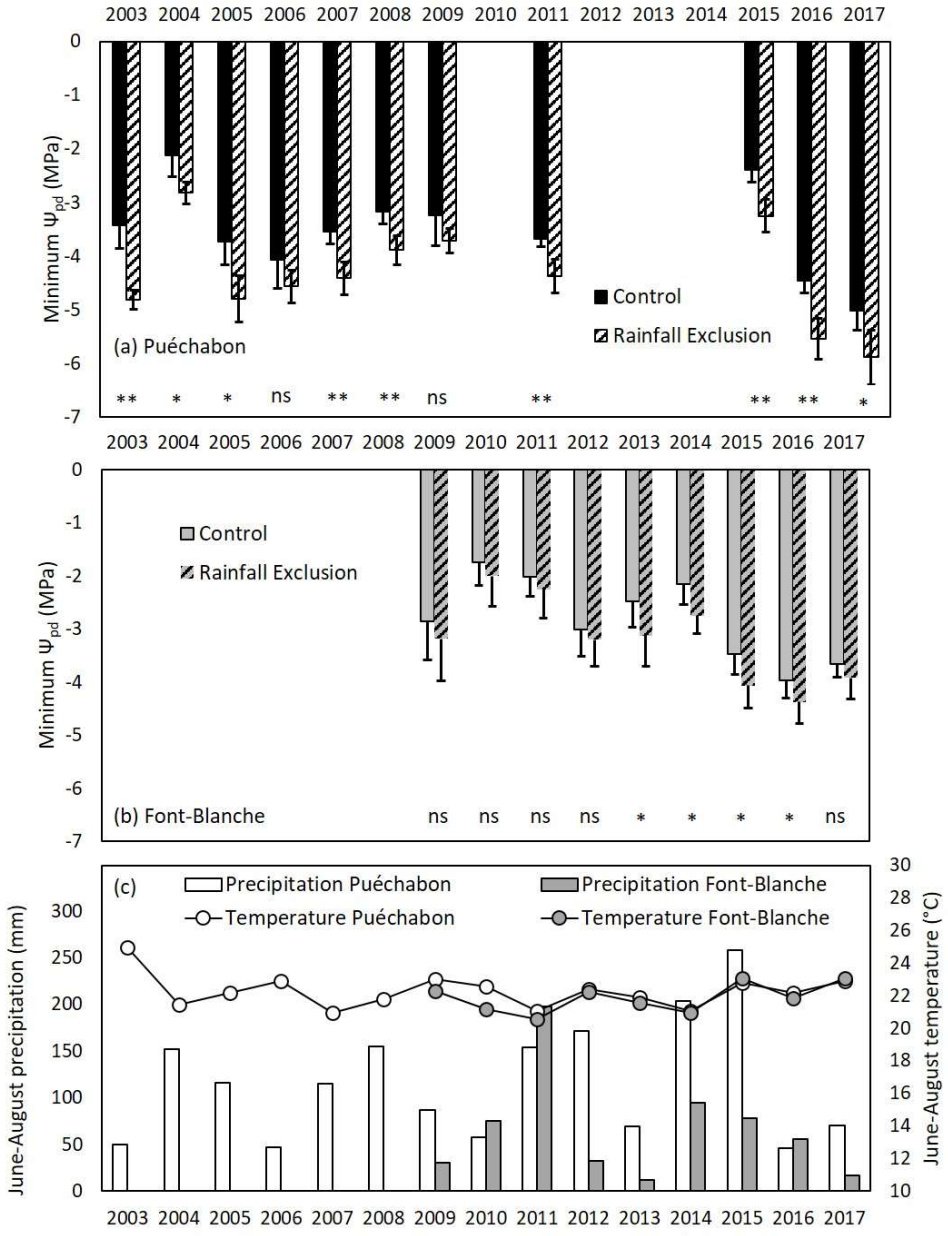

Fig. 1. Annual minimum values of predawn water potential (Ψ_{Pd}) measured in the control and rainfall exclusion treatments of the experiments of Puéchabon (a) and Font-Blanche (b) from the set-up of the experiments until 2017. Asterisks indicate significant differences between treatments at ** P<0.01; * P<0.05; ns non-significant. The panel (c) shows the inter-annual variations of precipitation and temperature during the summer months of June-July-August in the two forest sites.

Table 2. Metrics of the leaf water potential trajectories during soil drying derived from the relationships between Ψ_{Pd} and Ψ_{Md} measured in the field: the slope of the relationship between Ψ_{Md} and Ψ_{Pd}, the threshold at which $\Psi_{Md} = \Psi_{Pd}$, the minimum Ψ_{Md} when Ψ_{Pd}=0, and the area of the hydroscape. Values presented are the mean (±SE) per site and treatment, and the *P*-values of the ANOVA testing for Site and Treatment effects. Significant effects are in bold type with significance levels: * *P*<0.05; ** *P*<0.01; *** *P*<0.001.

		Slope Ψ_{Md} vs. Ψ_{Pd} (MPa Mpa^{-1})	$\Psi_{Md} = \Psi_{Pd}$ thres. (MPa)	Ψ_{Md} @ Ψ_{Pd} =0 (MPa)	Hydroscape (MPa^2)
Puéchabon	Control	0.552 (±0.017)	-4.20 (±0.19)	-2.43 (±0.12)	5.10 (±0.32)
	Rainfall excl.	0.570 (±0.020)	-4.31 (±0.18)	-2.31 (±0.09)	4.97 (±0.22)
Font-Blanche	Control	0.588 (±0.005)	-4.02 (±0.13)	-2.00 (±0.05)	4.02 (±0.18)
	Rainfall excl.	0.654 (±0.016)	-4.49 (±0.24)	-1.87 (±0.04)	4.18 (±0.15)
P-value	Site	**<0.001 *** **	0.978	**<0.001 *** **	**<0.001 *** **
	Treatment	**0.011 ***	0.146	0.145	0.925
	Site:Treatment	0.134	0.393	0.948	0.541

Table 3. Pressure-volume curve parameters per site and treatment: the osmotic potential at full turgor (Π_0), the water potential at the turgor loss point (Ψ_{tlp}), the relative water content at the turgor loss point (RWC_{tlp}), the mean modulus of elasticity (ε), and the apoplastic fraction (a_f). Values presented are the mean (±SE) per site and treatment, and the *P*-values of the ANOVA testing for Site and Treatment effects. Significant effects are in bold type with significance levels: * *P*<0.05; ** *P*<0.01; *** *P*<0.001.

		Π_0 (MPa)	Ψ_{tlp} (MPa)	RWC_{tlp} (%)	ε (MPa)	a_f (%)
Puéchabon	Control	-2.81 (±0.09)	-3.67 (±0.07)	86.8 (±1.6)	8.84 (±0.79)	44.2 (±2.9)
	Rainfall excl.	-3.08 (±0.17)	-4.12 (±0.15)	84.4 (±2.5)	10.27 (±1.19)	38.4 (±2.8)
Font-Blanche	Control	-2.52 (±0.12)	-3.65 (±0.17)	82.3 (±1.6)	7.08 (±0.51)	42.8 (±4.1)
	Rainfall excl.	-3.14 (±0.24)	-4.14 (±0.31)	83.7 (±2.2)	10.16 (±1.00)	31.0 (±5.7)
P-value	Site	0.43	0.88	0.27	0.33	0.32
	Treatment	**0.015 ***	**0.022 ***	0.75	**0.038 ***	**0.039 ***
	Site:Treat.	0.30	0.93	0.39	0.30	0.45

Shoot pressure-volume traits

The effect of the rainfall exclusion treatments on the pressure-volume (PV) traits was significant and similar in the two sites (no site × treatment interaction; Table 3). Trees growing in the rainfall exclusion treatments exhibited more negative osmotic potential at full turgor (Π_0) and more negative water potential at the turgor loss point (Ψ_{tlp}). The average treatment difference was approximately 0.45 MPa for both Π_0 and Ψ_{tlp}. The difference of approximately 1.00 MPa between Π_0 and Ψ_{tlp} remained constant independently of treatment. The mean modulus of elasticity (ε) and apoplastic fraction (a_f) also responded significantly to the treatments with larger values of ε and smaller values of a_f in the rainfall exclusion (Table 3). Conversely, the relative water content at the turgor loss point (RWC_{tlp}) did not change between

treatments and remained around 84%. No differences between sites were detected for any of the PV variables.

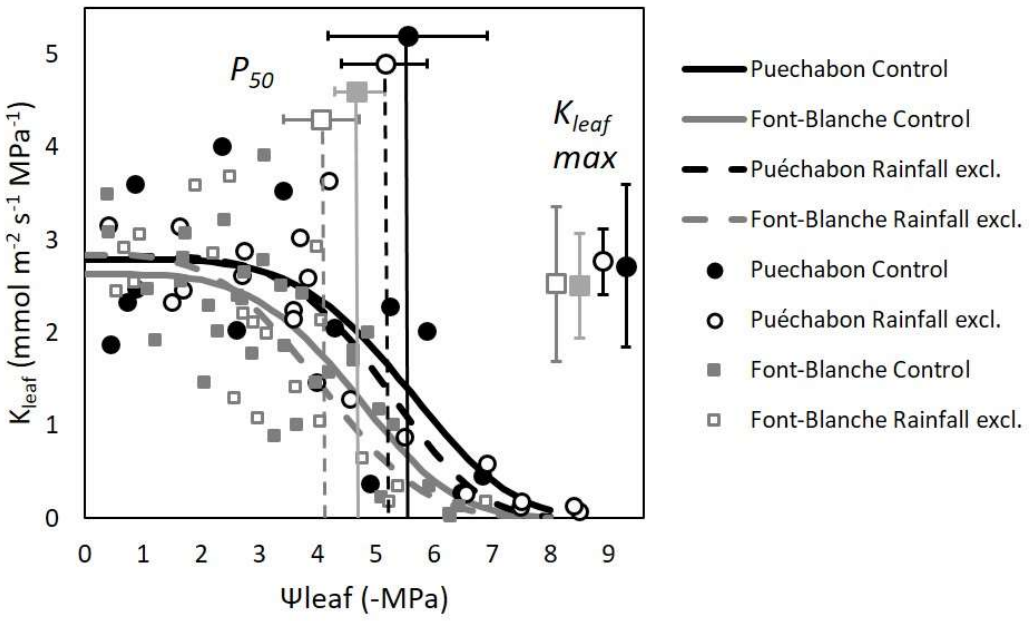

Fig. 2. Leaf vulnerability curves showing the relationship between K_{leaf} and Ψ_{leaf} for each site and treatment. Points represent the individual measurements and the curves are the fitted Weibull functions per treatment and site. The P_{50} and maximum K_{leaf} with their confidence intervals are shown at the top and on the right of the panel, respectively.

Leaf hydraulic conductance and vulnerability curve

The maximum leaf hydraulic conductance in well-hydrated branches ($K_{leaf,max}$) was around 2.63 (±0.13) mmol m^{-2} s^{-1} MPa^{-1} and did not differ significantly between either sites or treatments (P>0.35). K_{leaf} exhibited a significant decline with decreasing Ψ_{leaf}, with the Weibull function parameters being highly significant in every site and treatment (Fig. 2). The K_{leaf} P_{50} was significantly more negative in Puéchabon (-5.44 MPa ± 0.39) than in Font-Blanche (-4.41 MPa ± 0.19; P=0.027 for the site difference) but did not differ significantly between treatments (P=0.35 for the treatment difference). The K_{leaf} P_{12}, which bounds the range of Ψ_{leaf} in which there is no significant losses in K_{leaf}, did not differ significantly among sites and treatments and was on average -3.22 MPa ± 0.59. The K_{leaf} P_{88} did not differ significantly among sites and treatments either, and was on average -6.40 MPa ± 0.62. K_{leaf} and its relationship to water potential were thus similar among rainfall exclusion treatments in the two sites, with the rainfall exclusion treatments exhibiting slightly less negative values of K_{leaf} P_{12}, K_{leaf} P_{50} and K_{leaf} P_{88},

although differences were not statistically significant owing to the large variability of K_{leaf} among samples.

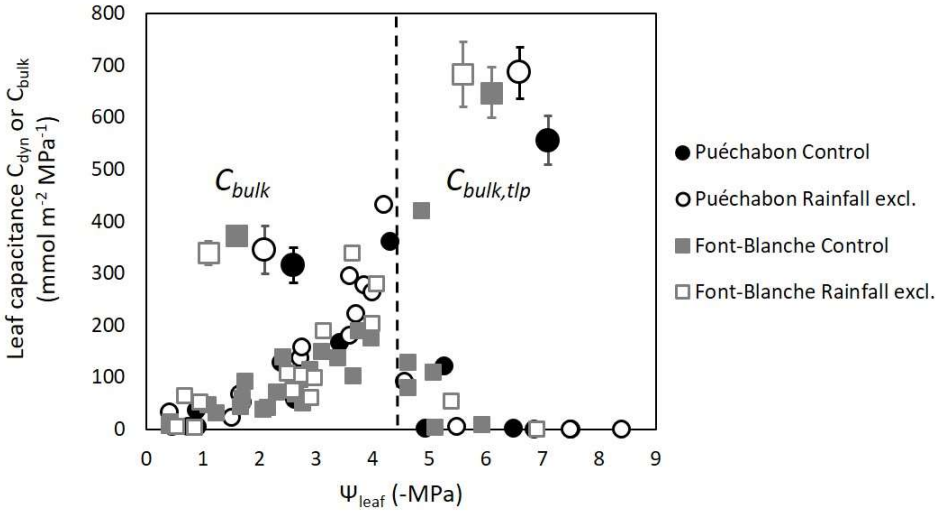

Fig. 3. Leaf hydraulic capacitance measured by rehydration (C_{dyn}) against Ψ_{leaf} for each site and treatment. The mean (±SE) of the bulk leaf capacitances calculated from the pressure-volume curves before (C_{bulk}, left side) and after the turgor loss ($C_{bulk,tlp}$, right side) are also shown with larger symbols and treatments arbitrary placed along the X-axis. The vertical dashed line indicates the apparent breakpoint in the C_{dyn} against Ψ_{leaf} relationship around -4.5 MPa.

Leaf mass per area, dry matter content and hydraulic capacitance

The *LMA* and *LDMC* did not change significantly with the rainfall exclusion treatments but exhibited slight differences among sites with a lower *LDMC* in Font-Blanche than in Puéchabon and a site × treatment interaction for *LMA* (Table S2). The bulk leaf capacitance (C_{bulk}) and bulk leaf capacitance after the turgor loss point ($C_{bulk,tlp}$) did not differ significantly among treatments or sites (Table S2, Fig. 3). The bulk leaf capacitance was around twice larger after the turgor loss point ($C_{bulk,tlp}$) than before (C_{bulk}). The hydraulic capacitance measured by the rehydration technique (C_{dyn}) exhibited a two-phase relationship with Ψ_{leaf} (Fig. 3). C_{dyn} increased significantly with decreasing Ψ_{leaf} until around -4.5 MPa ($P < 0.001$), and then decreased abruptly to very small values over the range of Ψ_{leaf} that causes a severe reduction of K_{leaf}. Values of C_{dyn} were generally lower than C_{bulk}, although they reached a similar range of variation at Ψ_{leaf} around -4.0 MPa (Fig. 3). No statistical difference in C_{dyn} was detected among sites and treatments (Table S2).

Table 4. Leaf gas-exchange conductance: minimum conductance to water vapor (g_{min}), stomatal conductance to water vapor (g_s) and mesophyll conductance to CO_2 (g_m) measured under well-watered conditions. Values presented are the mean (±SE) per site and treatment, and the *P*-values of the ANOVA testing for Site and Treatment effects, or the Student's t-test for Treatment effect when measurements were only available in one site. Significant effects are in bold type with significance levels: * $P<0.05$; ** $P<0.01$; *** $P<0.001$.

		g_{min} (mmol m^{-2} s^{-1})	g_s (mmol m^{-2} s^{-1})	g_m (mmol CO_2 m^{-2} s^{-1})
Puéchabon	Control	3.84 (±0.20)	106.1 (±9.5)	117.6 (±16.9)
	Rainfall excl.	3.86 (±0.33)	68.6 (±7.7)	75.5 (±6.7)
Font-Blanche	Control	3.05 (±0.08)		
	Rainfall excl.	3.85 (±0.41)		
P-value	Site	0.194		
	Treatment	0.213	**0.017** *	0.058
	Site:Treatment	0.210		

Leaf minimum, stomatal and mesophyll conductance

The average leaf minimum conductance to water vapor (g_{min}) was between 3 and 4 mmol m^{-2} s^{-1} and did not differ significantly between sites or treatments (Table 4). Conversely, the stomatal conductance to water vapor (g_s) measured in Puéchabon in autumn 2017, a few months before the leaf sampling and after drought relief by the autumn rain (86 mm over the preceding month in the control treatment), was significantly lower in the rainfall exclusion treatment than in the control (P=0.017, Table 4). The mesophyll conductance to CO_2 (g_m) measured concomitantly exhibited a similar response to rainfall exclusion than g_s, although the difference between treatments was only marginally significant (P=0.058).

Correlations among traits

Coordination among traits was observed, on the one hand, among the traits derived from the PV-curves and, on the other hand, among the traits derived from water potential measurements, but surprisingly these two groups were not related to each other or to gas-exchange traits (Table 5; Fig. S3). Coordination among the PV-curve traits revealed that Ψ_{tlp} was strongly correlated with both Π_0 and a_f but not with ε. RWC_{tlp} was correlated with both ε and a_f but not with Π_0. Consequently, Ψ_{tlp} was more negative in leaves with a more negative osmotic potential Π_0 or with a smaller fraction of apoplastic water (lower a_f), and RWC_{tlp} was higher in leaves with more rigid cell walls (larger ε) or less water in the symplasm (larger a_f).

Leaf capacitance before and after turgor loss, C_{bulk} and $C_{bulk,tlp}$, were not correlated and were related differently to the other leaf traits. Leaves with a higher *LDMC* had a lower capacitance before turgor loss (C_{bulk}) and kept a larger RWC_{tlp}. The leaf capacitance after turgor loss ($C_{bulk,tlp}$) was larger in leaves with a larger LMA and a larger fraction of symplastic water (smaller a_f).

Traits derived from the relationship between Ψ_{Pd} and Ψ_{Md} also exhibited some coordination (Table 5; Fig. S3). Trees with a more anisohydric behavior (steeper slope) had generally a more negative threshold at which predawn and midday water potential become equal ($\Psi_{Md} = \Psi_{Pd}$) but also a less negative Ψ_{Md} when Ψ_{Pd} is equal to zero (Ψ_{Md} @ Ψ_{Pd}=0). The hydroscape area was mainly driven by Ψ_{Md}@Ψ_{Pd}=0 and was larger in leaves with a high *LDMC*.

Remarkably, we observed no correlation between any of the PV-curve traits and the gas-exchange traits or the hydroscape traits (Table 5; Fig. S3), so we could not identify any relationship at the tree scale between the leaf water potential trajectories observed in the field and the water relations derived from the PV curves. The *LMA* was a very poor predictor of leaf water relations as it was only related to $C_{bulk,tlp}$. Finally, we observed a positive correlation between g_s and the threshold at which predawn and midday water potential become equal ($\Psi_{Md} = \Psi_{Pd}$), so that trees with a higher g_s under well-watered conditions tended to stop transpiring earlier during drought, and conversely.

Sequence of leaf responses to dehydration

The sequence of leaf responses to progressively decreasing Ψ_{leaf} followed the order 'Ψ_{Md}@Ψ_{Pd}=0' > 'K_{leaf} P_{12}' ≥ 'Ψ_{tlp}' > 'Ψ_{Md}=Ψ_{Pd}' > 'K_{leaf} P_{50}' > 'K_{leaf} P_{88}', in the control treatment (Fig. 4). This order was generally conserved among treatments and among sites, although the significance of the differences between traits varied (Fig. 4; Fig. S4). This sequence shows that under non water-limited conditions, the stomatal regulation maintains Ψ_{Md} above the thresholds for the loss of K_{leaf} (K_{leaf} P_{12}) or the loss of turgor (Ψ_{tlp}). When drought occurs and Ψ_{leaf} decreases further, we found K_{leaf} P_{12} and Ψ_{tlp} to occur almost concomitantly, although with a non-significant tendency for less negative K_{leaf} P_{12} than Ψ_{tlp}. The leaf water potential at which Ψ_{Md}=Ψ_{Pd} in the field was more negative than the measured Ψ_{tlp}. Finally, the severe losses of K_{leaf} (K_{leaf} P_{50} and K_{leaf} P_{88}) were the last consequences of decreasing Ψ_{leaf}.

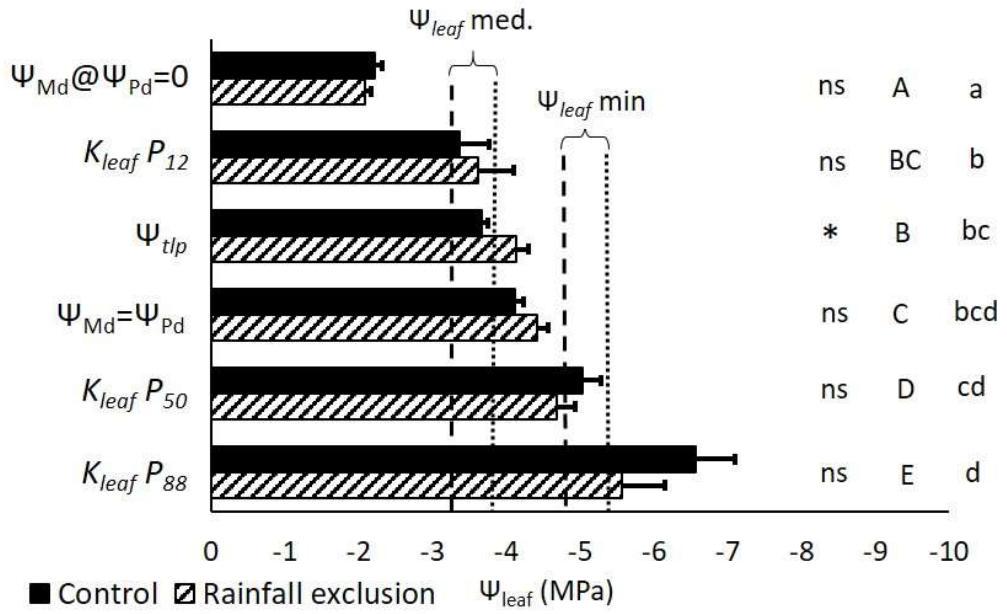

Fig. 4. Sequence of leaf water potential values for the different traits describing leaf tolerance to drought in the control and rainfall exclusion treatments of the two experimental sites. $\Psi_{Md}@\Psi_{Pd}=0$ is the minimum Ψ_{Md} when Ψ_{Pd} is equal to zero, $K_{leaf}\,P_{12}$ is the Ψ_{leaf} threshold for K_{leaf} loss, Ψ_{tlp} is the water potential at the turgor loss point, $\Psi_{Md}=\Psi_{Pd}$ is the water potential at which predawn and midday water potential become equal, $K_{leaf}\,P_{50}$ is the Ψ_{leaf} value inducing a 50% loss of K_{leaf}, and $K_{leaf}\,P_{88}$ corresponds to the Ψ_{leaf} value inducing an 88% loss of K_{leaf}. Error bars are standard error, * and 'ns' on the right side of the figure indicate for each trait whether the difference between the control and the rainfall exclusion treatments was significant at $P<0.05$. Different upper case letters indicate significant differences between traits of the sequence in the control treatment, and different lower case letters indicate significant differences between traits of the sequence in the rainfall exclusion treatment. Median and absolute minimum values of Ψ_{Pd} recorded in the field during drought (Ψ_{leaf} med. , Ψ_{leaf} min) are also indicated by dashed lines for the control treatment, and by dotted lines for the rainfall exclusion treatment.

The differences between $\Psi_{Md}@\Psi_{Pd}=0$ and $K_{leaf}\,P_{12}$ or Ψ_{tlp} were larger, on average, in the rainfall exclusion than in the control treatments ($\Psi_{Md}@\Psi_{Pd}=0$ minus $K_{leaf}\,P_{12}$: 1.14 ± 0.42 MPa *vs.* 1.53 ± 0.49 MPa for the control and rainfall exclusion treatments, respectively; $\Psi_{Md}@\Psi_{Pd}=0$ minus Ψ_{tlp}: 1.44 ± 0.12 MPa *vs.* 2.06 ± 0.17 MPa for the control and rainfall exclusion treatment, respectively; Fig. 4) indicating that, under well-watered conditions, the trees from the rainfall exclusion treatments kept a larger margin before possibly losing some K_{leaf} or cell turgor. However, some differences between traits along the sequence tended to be reduced and less significant in the rainfall exclusion treatments due to both more negative Ψ_{tlp} and less negative $K_{leaf}\,P_{50}$. As a consequence, the events of $K_{leaf}\,P_{12}$, Ψ_{tlp}, $\Psi_{Md}=\Psi_{Pd}$ and $K_{leaf}\,P_{50}$ all tended to occur within a narrower range of Ψ_{leaf} in the rainfall exclusion treatment (Fig. 4). The difference between $\Psi_{Md}=\Psi_{Pd}$ and $K_{leaf}\,P_{50}$ was reduced in the rainfall exclusion treatment (0.91 ± 0.28

MPa *vs.* 0.27 ± 0.29 MPa for the control and rainfall exclusion treatment, respectively) so the trees growing in drier conditions kept a narrower margin between the cessation of transpiration under severe water stress and the loss of leaf hydraulic function. The minimum Ψ_{leaf} measured in the rainfall exclusion treatments have exceeded the trees K_{leaf} P_{50} at least once since the start of the experiments in both Puéchabon and Font-Blanche, but this has never been the case yet in the control treatments (Fig. 4; Fig. S4). The median yearly minimum Ψ_{leaf} measured in the field show that the trees from the rainfall exclusion treatments exceed the K_{leaf} P_{12} at least every other year, while they do not reach this threshold as often in the control treatments. Thresholds Ψ_{tlp} and Ψ_{Md}=Ψ_{Pd} were slightly more negative than the median Ψ_{Pd} in every site and treatment, except in the rainfall exclusion treatment in Puéchabon (Fig. S4).

Table 5. Pearson correlation matrix among the different traits measured in each tree for all sites and treatments pooled together (*n*=26 trees for traits measured in the laboratory on PV curve samples, and *n*=17 trees for 'hydroscape' traits or *n*=12 trees for gas-exchange traits measured in the field). The name of the variables are the same as in the other tables. Significant effects are in bold type with significance levels: * $P<0.05$; ** $P<0.01$; *** $P<0.001$.

	Ψ_{tlp}	Π_0	ε	a_f	RWC_{tlp}	C_{bulk}	$C_{bulk,tlp}$	LMA	LDMC	Sl. Ψ_{Md} vs. Ψ_{Pd}	$\Psi_{Md} = \Psi_{Pd}$ thres.	Ψ_{Md} @ Ψ_{Pd} =0	Hydrosc.	g_s	g_m
Π_0	**0.77** ***														
ε	-0.29	**-0.76** ***													
a_f	**0.79** ***	**0.63** ***	-0.29												
RWC_{tlp}	**0.47** *	-0.17	**0.49** *	**0.51** **											
C_{bulk}	-0.10	**0.47** *	**-0.61** **	-0.22	**-0.84** ***										
$C_{bulk,tlp}$	-0.35	**-0.55** **	**0.59** **	**-0.53** **	0.08	-0.11									
LMA	-0.21	-0.23	0.17	-0.05	0.03	0.06	**0.51** **								
LDMC	-0.06	-0.36	0.26	0.16	**0.48** *	**-0.52** **	-0.12	0.21							
Slope Ψ_{Md} vs. Ψ_{Pd}	-0.45	-0.35	0.18	-0.36	-0.05	-0.04	0.44	-0.01	-0.18						
$\Psi_{Md} = \Psi_{Pd}$ thres.	0.22	0.08	-0.16	0.04	-0.14	0.20	-0.26	-0.03	-0.27	**-0.65** **					
Ψ_{Md} @ Ψ_{Pd} =0	-0.33	-0.26	0.18	-0.36	-0.08	0.10	0.46	-0.13	-0.43	**0.88** ***	-0.40				
Hydroscape	0.15	0.19	-0.06	0.34	0.20	-0.26	-0.28	0.16	**0.65** **	-0.42	-0.33	**-0.72** **			
g_s	0.36	0.54	-0.41	-0.07	-0.41	0.36	-0.42	-0.37	-0.21	-0.53	**0.66** *	-0.18	-0.35		
g_m	0.27	0.49	-0.45	0.01	-0.38	0.39	-0.28	**-0.54** *	-0.38	-0.03	0.19	0.32	-0.41	**0.68** *	
g_{min}	-0.35	-0.23	0.22	-0.19	-0.19	0.18	-0.12	0.18	0.18	-0.27	0.28	-0.21	0.06	-0.02	-0.23

Discussion

Leaf hydraulic traits do not acclimate to long-term increased aridity

The two rainfall exclusion experiments implemented in Puéchabon and Font-Blanche were efficient in increasing recurrently the water stress experienced by the trees (Fig. 1), but none of them resulted in significant changes of the leaf hydraulic vulnerability to water stress between the control and rainfall exclusion treatments (Fig. 2). Such an absence of plastic response to experimentally increased drought seems to confirm for the leaf hydraulics what was previously observed in similar experiments for branch hydraulic plasticity (Limousin *et al.* 2010; Hudson *et al.* 2018). Although plastic adjustments of the hydraulic vulnerability to water stress would be a powerful mean of acclimation to drought, there has yet been limited evidence for it in tree species. Some authors have observed a plastic response towards a lower xylem hydraulic vulnerability in experimentally water stressed trees, but this finding was generally restricted to seedlings and to particular species or ecotypes (Ladjal *et al.* 2005; Beikircher and Mayr 2009; Awad *et al.* 2010; Fichot *et al.* 2010; Corcuerra *et al.* 2011). Conversely, studies using reciprocal transplants have observed a limited plasticity of the branch hydraulic vulnerability, and unexpectedly more vulnerable xylem in the drier sites (Wortemann *et al.* 2011; Lamy *et al.* 2014).

Leaves are expected to exhibit a greater potential for hydraulic plasticity than branches, because K_{leaf} involves both a xylem pathway in the leaf veins and an outside-xylem pathway in the mesophyll (Cochard *et al.* 2004; Scoffoni and Sack 2017). The K_{leaf} decrease with water stress may be driven by xylem embolism (Brodribb *et al.* 2016), but also by leaf and cell shrinkage following dehydration (Scoffoni *et al.* 2014), decreased aquaporin activity (Kim and Steudle 2007, Shatil-Cohen *et al.* 2011), or a combination of all the above (Trifilo *et al.* 2016; Scoffoni and Sack 2017). A seasonal acclimation of K_{leaf} has been observed in grapevines with decreasing K_{leaf} P_{50} while drought progresses (Martorell *et al.* 2015; Sorek *et al.* 2020). Martorell *et al.* (2015) hypothesized that such a drought acclimation was related to seasonal osmotic adjustments that maintain cell turgor and prevent leaf shrinkage thereby favoring hydraulic conductance in the outside-xylem pathway and aquaporin activity. More recent evidence suggests, however, that the seasonal plasticity of K_{leaf} P_{50} in grapevines is mostly related to xylem anatomical changes occurring through leaf ontogeny and maturation and is

little influenced by drought intensity (Sorek *et al.* 2020), a phenomenon that has also been described for stem hydraulic vulnerability in this particular species (Charrier *et al.* 2018).

Here we performed our measurements in an evergreen species, on 1-year old leaves that had endured a severe drought stress the preceding summer, several months before sampling (Fig. 1). Significant changes in $K_{leaf,max}$ and K_{leaf} P_{50} were thus to be expected between treatments and sites according to several alternative hypotheses: (hyp. 1) K_{leaf} would have acclimated to seasonal drought in proportion to treatment differences in Ψ_{tlp}, similarly to what is observed in grapevines (Martorell *et al.* 2015; Sorek *et al.* 2020); (hyp. 2) drought induced embolism in the leaf xylem would vary with the minimum Ψ_{leaf} experienced the previous summer, and would either lower $K_{leaf,max}$ and K_{leaf} P_{50} in the rainfall exclusion treatments (Cochard *et al.* 2013), or alternatively would increase K_{leaf} P_{50} due to cavitation fatigue (Hacke *et al.* 2001); (hyp. 3) partial leaf drying and shedding observed in Puéchabon in 2017 as a consequence of the extreme water stress (Martin-StPaul *et al.* 2020) would have selected the most hydraulically resistant leaves in this site.

The K_{leaf} P_{50} measured in our study, with values between -4.41 MPa and -5.44 MPa, was more negative than values already reported in *Q. ilex* (K_{leaf} P_{50} = -3.5 MPa in Nardini *et al.* 2012) or in other oak species (range of K_{leaf} P_{50} between -2.0 MPa and -3.5 MPa in evergreen and deciduous oaks measured in: Brodribb and Holbrook 2003; Scoffoni *et al.* 2011; Johnson *et al.* 2012; Nardini *et al.* 2012; Trifilo *et al.* 2016; Scoffoni *et al.* 2017). $K_{leaf,max}$ was also lower than values previously reported in these studies where they generally range between 4 and 11 mmol m^{-2} s^{-1} MPa^{-1} in oak species. Besides confirming that K_{leaf} is particularly drought resistant in *Q. ilex* (Nardini *et al.* 2012; Nardini and Luglio 2014), this result is coherent with the fact that our measurements were performed on old and drought-hardened leaves. Interestingly, the leaves were nonetheless more vulnerable to drought than branch xylem. We find a difference of more than 1 MPa between K_{leaf} P_{50} and the stem xylem P_{50} reported in the literature for *Q. ilex*, with K_{leaf} P_{50} being more in the range of stem P_{12} (Lobo *et al.* 2018; Sergent *et al.* 2020). This supports the vulnerability segmentation hypothesis according to which leaves may act as a 'safety-valve' protecting the branches from xylem embolism during severe water stress (Tyree and Ewers 1991; Zhu *et al.* 2016; Scoffoni and Sack 2017), and is in accordance with observations of widespread leaf browning and shedding in Puéchabon during the severe 2016 and 2017 droughts while branch mortality remained very limited (Martin-StPaul *et al.* 2020).

In our study, intra-specific variability in leaf hydraulic traits was only detected between sites for K_{leaf} P_{50}, which was more negative in Puéchabon where the lowest Ψ_{Pd} were measured (Fig.

1; Fig. 2). Nevertheless, the absence of treatment effect on $K_{leaf,max}$ and K_{leaf} P_{50} (Fig. 2) contradicts the three hypotheses mentioned above, because differences between sites may have a genetic origin or be driven by plastic responses to other environmental factors than drought. Rejecting hyp. 1 suggests that, in *Q. ilex*, the drought acclimation of K_{leaf} P_{50} is more limited than the plasticity of other leaf and plant traits, especially those derived from PV curves. Rejecting hyp. 2 suggests that losses of K_{leaf} during the severe water stress in 2017 were mostly reversible. This interpretation is consistent with reports that the outside-xylem component drives most of the K_{leaf} vulnerability in other drought resistant oak species such as *Q. rubra* (deciduous, Trifilo *et al.* 2016) and *Q. agrifolia* (evergreen, Scoffoni *et al.* 2017), and with reports that xylem vulnerability to cavitation in *Q. ilex* is more negative than leaf water potentials observed in 2017 (between -6.30 and -7.16 MPa for xylem P_{50} in branches, Sergent *et al.* 2020; -6.40 MPa for xylem P_{50} in leaves, Moreno *et al.* in prep). However, K_{leaf} measurements before drought exposure would have been necessary to verify the absence of permanent K_{leaf} losses. Finally, rejecting hyp. 3 suggests a limited variability of K_{leaf} P_{50} within individuals, at least among the top-canopy sun-exposed leaves. Investigating the seasonal variations in leaf hydraulics during drought progression would now be necessary to better understand the roles of hydraulic plasticity and leaf aging in drought acclimation.

Leaf drought tolerance acclimates through osmotic adjustments

Contrary to hydraulic traits, PV-derived traits Ψ_{tlp}, Π_0, ε and a_f all exhibited a significant plasticity in response to experimental rainfall manipulation (Table 3). Trees growing in the rainfall exclusion treatments had a more negative Ψ_{tlp} than trees in the control treatments, thereby allowing the leaves to maintain cell turgor under drier soil conditions. This plastic adjustment is a common and expected drought response, particularly in anisohydric (Meinzer *et al.* 2014) and Mediterranean species (Bartlett *et al.* 2014) such as *Q. ilex*. The average 0.47 MPa difference in Ψ_{tlp} between treatments was very similar to the mean seasonal plasticity in turgor loss point evidenced in a meta-analysis of 283 species (0.44 MPa; Bartlett *et al.* 2014). The Ψ_{tlp} response to rainfall exclusion was driven by osmotic adjustment, as evidenced by the strong correlation between Ψ_{tlp} and Π_0 (Table 5) and by the comparable magnitude of change between treatments for Π_0 (0.45 MPa) and for Ψ_{tlp} (0.47 MPa; Table 3). This finding is consistent with strong empirical and theoretical evidence that changes in Ψ_{tlp} within and across species are mainly driven by changes in Π_0 rather than ε (Lenz *et al.* 2006; Bartlett *et al.* 2012).

Leaf acclimation to drought through osmotic adjustment arises from the accumulation of solutes such as sugars, amino-acids and ions in the cells that lower Π_0 during periods of drought (Morgan 1984). Osmotic adjustment is energetically costly because these solutes become unavailable for growth and metabolism (Bartlett *et al.* 2014; Salmon *et al.* 2015). On the other hand, growth and metabolism are also down-regulated during drought (Rodriguez-Calcerrada *et al.* 2011; Lempereur *et al.* 2015), which reduces the sink of sugars and amino-acids and thus the cost of osmotic adjustment. Although some studies have reported that osmotic adjustment may be rapidly reversed upon leaf rehydration (Davis and Mooney 1986; Thomas and Gausling 2000), others have shown that leaves can maintain more negative Π_0 and Ψ_{tlp} for long periods of time after the return of wetter conditions (Hsiao *et al.* 1976). This is particularly the case in *Q. ilex* which presents significantly more negative Π_0 and Ψ_{tlp} in drought-hardened 1-year old leaves than in newly emerged leaves before their first exposure to drought (Dreyer *et al.* 1990). This drought legacy explains why rainfall exclusion effects on Π_0 and Ψ_{tlp} were maintained in spring 2018, in a period when experimental rainfall exclusion had no impact on tree Ψ_{pd}. Leaf osmotic adjustment thus appears as a powerful mechanism to cope with water stress but also to acclimate to repeated drought cycles in species where lower Π_0 can be sustained through time (Bartlett *et al.* 2014).

Although ε and a_f also exhibited a significant treatment response in our study (Table 3), these two traits could not contribute to lower Ψ_{tlp} in the rainfall exclusion treatment because their variation was in the opposite direction than that driving a causal decrease of Ψ_{tlp} according to the PV curve theory (Bartlett *et al.* 2012). Mechanistically, a higher ε and a lower a_f should drive less negative Ψ_{tlp}, contrary to what we observed here. Hence, plastic adjustments of ε and a_f in response to the rainfall exclusion should rather be interpreted for their effects on RWC_{tlp} and leaf capacitance because a coordinated reduction of Π_0 and increase of ε allows to lower Ψ_{tlp} while maintaining a constant RWC_{tlp}. This coordinated response, known as the 'cell water conservation hypothesis' (Cheung *et al.* 1975; Bartlett *et al.* 2012), prevents the dangerous cell dehydration and shrinkage that could otherwise arise from lowering the Ψ_{tlp}. As a matter of fact, RWC_{tlp} was the only invariable PV curve trait in our results (Table 3), which highlights the importance of conserving cell water while osmotically acclimating to drought. Likewise, higher ε and lower a_f were correlated with an increase in $C_{bulk,tlp}$ (Table 5, Bartlett *et al.* 2012). This plastic response contributes to the ability to survive water shortage because $C_{bulk,tlp}$ determines the leaf water storage available after turgor loss and stomatal closure, and thus the leaf survival time before complete desiccation (Sack *et al.* 2003). However, in spite of significant treatment

effects on a_f and ε, the observed increase in $C_{bulk,tlp}$ in the rainfall exclusion treatments was not large enough to be significant (Table S2). Moreover, because we did not observe any change in g_{min} between treatments (Table 4), we only have indirect indication that acclimation to drought in the rainfall exclusion treatments allows the leaves to withstand longer drought periods before desiccation.

Acclimation of drought tolerance is associated with narrower safety margins

The plastic responses of the Ψ thresholds for leaf functional decline during drought did not modify their sequence between treatments and sites (Fig. 4; Fig. S4). Our results mostly confirmed earlier conclusions obtained in meta-analysis or species comparison, with a notable exception being the rank of K_{leaf} P_{50} which was more negative than Ψ_{tlp} and the water potential at complete stomatal closure (assessed by Ψ_{Md}=Ψ_{Pd}), contrary to what is generally reported in other species (Bartlett *et al.* 2016; Trueba *et al.* 2019). This difference is likely explained by the evergreen phenology of *Q. ilex*, as evergreen leaves must avoid hydraulic dysfunction in order to remain functional for several years (Bartlett *et al.* 2016). This result, and the fact that Ψ_{Md}@Ψ_{Pd}=0 was significantly less negative than K_{leaf} P_{12}, indicate that the loss of leaf hydraulic conductance, whether inside or outside the xylem, does not occur routinely in *Q. ilex* leaves and is avoided by stomatal regulation under well-watered to moderately water stressed conditions (Creek *et al.* 2020).

Our study is the first to investigate experimentally the impact of plasticity on this sequence of drought tolerance thresholds. Ψ_{tlp} exhibited a significant plasticity in response to the experimental treatments, and non-significant changes toward more negative Ψ values were observed for K_{leaf} P_{12} and Ψ_{Md}=Ψ_{Pd}, and toward less negative Ψ values for Ψ_{Md}@Ψ_{Pd}=0, K_{leaf} P_{50} and K_{leaf} P_{80} (Fig. 4). The consequence of plasticity was thus a small contraction of the safety margins because K_{leaf} P_{12}, Ψ_{tlp}, Ψ_{Md}=Ψ_{Pd} and K_{leaf} P_{50} all occurred within a narrower range of Ψ_{leaf} in the rainfall exclusion treatment than in the control. Our results thus support the view of Martin-StPaul *et al.* (2017) that drought acclimation increases the risk of hydraulic failure, because a more negative Ψ_{tlp} in drought-acclimated leaves promotes latter stomatal closure during drought (Brodribb and Holbrook 2003; Martin-StPaul *et al.* 2017). The leaf water potential at complete stomatal closure under field conditions should, however, be more accurately quantified by Ψ_{Md}=Ψ_{Pd} than by Ψ_{tlp} (Meinzer *et al.* 2016). Although, Ψ_{tlp} and stomatal closure generally match in interspecific studies (Meinzer *et al.* 2016; Martin-StPaul *et*

al. 2017), results in our control treatments confirm the observation by Bartlett *et al.* (2016) that Ψ_{leaf} at complete stomatal closure in the field (here $\Psi_{Md}=\Psi_{Pd}$) can be significantly more negative than Ψ_{tlp} (Fig. 4). This difference may be explained either by a larger seasonal plasticity in Ψ_{tlp} than what we quantified here with our treatment comparison, or by the fact that guard cells controlling stomatal aperture are partly isolated from the bulk leaf turgor (Buckley 2019). In any case, considering either $\Psi_{Md}=\Psi_{Pd}$ or Ψ_{tlp} as thresholds for stomatal closure confirms that leaf safety margins before hydraulic failure were smaller in the rainfall exclusion than in the control treatments.

The trajectories of Ψ_{Md} regulation exhibited a limited plasticity between treatments, which points out nevertheless to a more anisohydric behavior in the rainfall exclusion treatments (steeper Slope Ψ_{Md} vs. Ψ_{Pd}; Table 2). Moreover, anisohydry was associated with more negative $\Psi_{Md}=\Psi_{Pd}$ and less negative $\Psi_{Md}@\Psi_{Pd}=0$ (Table 2). A more anisohydric regulation of Ψ_{Md} has thus two consequences: first, complete stomatal closure tends to occur later under drought, which reduces the safety margin before hydraulic failure; second, a larger difference is maintained between Ψ_{Md} and K_{leaf} P_{12} or Ψ_{tlp} under well-watered conditions. This smaller diurnal drop in Ψ_{Md} under well-watered conditions in the rainfall exclusion treatments is consistent with observations that more negative Π_0 is generally correlated with lower maximum stomatal conductance (Henry *et al.* 2019; Bartlett and Sinclair 2020). It is also consistent with previous observations that tree hydraulic architecture has acclimated through a reduced leaf area per sapwood area in the rainfall exclusion treatments, which, in turn, reduces the tree transpiration and water potential gradient from the soil to the leaves (Limousin *et al.* 2010a; Martin-StPaul *et al.* 2013; Moreno *et al.* 2021).

These results collectively suggest an acclimation of leaf gas-exchange regulation in the rainfall exclusion treatments, which involves both a more negative Ψ_{leaf} threshold for stomatal closure under drought but also a lower transpiration and Ψ_{leaf} drop under well-watered conditions. This pattern of drought acclimation is further suggested by the positive correlation observed between g_s and $\Psi_{Md}=\Psi_{Pd}$ (Table 5). This means that trees with a latter stomatal closure during drought also exhibit a lower maximum transpiration in well-watered periods, and conversely, a phenomenon previously described in conifer species exposed to a long-term rainfall exclusion experiment (Limousin *et al.* 2013). By delaying the stomatal closure and the turgor loss during drought progression, leaf acclimation to drought would thus benefit tree functioning mostly in periods of moderate water stress. This is consistent with an earlier observation that increased stem hydraulic capacitance in the rainfall exclusion treatment in Puéchabon contributed to

carbon gain during well-hydrated periods, rather than to prevent losses of hydraulic conductance during severe water stress (Salomon *et al.* 2020). From a gas-exchange perspective, these responses to rainfall exclusion allow the maintenance of a positive leaf carbon balance for longer periods and the maximization of the water use efficiency (Holloway-Phillips and Brodribb 2011; Limousin *et al.* 2013). Perhaps more importantly in the evergreen *Q. ilex*, drought acclimation may also maintain the turgor necessary for growth during longer periods of time (Lempereur *et al.* 2015), and the source of photo-assimilates necessary to the initiation of future organs in buds and the accumulation of reserves in seeds, two processes that occur during the water limited summer (Bykova *et al.* 2018; Le Roncé *et al.* 2020). Such an increased tolerance to moderate drought seems however to be a risky behavior in case of severe drought as it does not increase the leaf resistance to severe water stress.

Acknowledgments

The authors thank Eric Badel, Nicolas Barthès, Lise-Marie Billon, Damien Gounelle, Arnaud Jouineau, Nicolas Mariotte, Alexandru Milcu and Karim Piquemal for their help in the field and the lab over the course of these experiments. The Puéchabon and Font-Blanche experimental sites both belong to the French national research infrastructure ANAEE-France (ANR-11-INBS-0001) and the French network of ICOS Ecosystem stations (Integrated Carbon Observation System ERIC). Puéchabon is further supported by the OSU OREME (UMS 3282). J R-C acknowledges the Spanish Mobility Program "José Castillejo" and M M a PhD scholarship from the French Environment and Energy Management Agency (ADEME). This research was further supported by the Agence Nationale pour la Recherche (project Drought+ ANR-06-VULN-003-04; project HydrauLeaks ANR-18-CE20-0005).

Authors Contribution

JML and NMS conceived and designed the study; JML, LGJ, JMO, GS and NMS collected the data in the field; AR, MM, JRC, JMTR and HC performed the lab measurements, AR, JML and NMS analyzed data; JML led the writing. All authors contributed critically to results interpretation and drafts of the manuscript.

Conflict of Interest

No conflict of interest to declare.

Data Availability

The data that support the findings of this study are available from the corresponding author upon reasonable request.

References

Adams HD, Zeppel MJB, Anderegg WRL, Hartmann H, Landhauser SM, Tissue DT, Huxman TE, Hudson PJ, Franz TE, Allen CD, *et al.* (2017) A multi-species synthesis of physiological mechanisms in drought-induced tree mortality. *Nature Ecology & Evolution*, **1**, 1285-1291

Allen CD, Macalady AK, Chenchouni H, Bachelet D, McDowell N, Vennetier M, Ktizberger T, Rigling A, Breshears DD, Hogg EH, Gonzalez P, Fensham R, Zhang Z, Castro J, Demidova N, Lim JH, Allard G, Running SW, Semerci A, Cobb N (2010) A global overview of drought and heat-induced tree mortality reveals emerging climate change risks for forests. *Forest Ecology and Management*, **259**, 660-684

Anderegg WRL, Klein T, Bartlett M, Sack L, Pellegrini AFA, Choat B, Jansen S (2016) Meta-analysis reveals that hydraulic traits explain cross-species patterns of drought-induced tree mortality across the globe. *PNAS*, **113**, 5024-5029

Awad H, Barigah T, Badel E, Cochard H, Herbette S (2010) Poplar vulnerability to xylem cavitation acclimates to drier soil conditions. *Physiologia Plantarum*, **139**, 280-288

Bartlett MK, Klein T, Jansen S, Choat B, Sack L (2016) The correlations and sequence of plant stomatal, hydraulic, and wilting responses to drought. *PNAS*, **113**, 13098-13103

Bartlett MK, Scoffoni C, Sack L (2012) The determinants of leaf turgor loss point and prediction of drought tolerance of species and biomes: a global meta-analysis. *Ecology Letters* **15**,393–405

Bartlett MK, Sinclair G (2021) Temperature and evaporative demand drive variation in stomatal and hydraulic traits across grape cultivars. *Journal of Experimental Botany*, **72**, 1995-2009

Bartlett MK, Zhang Y, Kreidler N, Sun S, Ardy R, Cao K, Sack L (2014) Global analysis of plasticity in turgor loss point, a key drought tolerance trait. *Ecology Letters*, **17**, 1580-1590

Beikircher B, Mayr S (2009) Intraspecific differences in drought tolerance and acclimation in hydraulics of *Ligustrum vulgare* and *Viburnum lantana*. *Tree Physiology*, **29**, 765-775

Bernacchi CJ, Portis Jr AR, Nakano H, von Caemmerer S, Long SP (2002) Temperature Response of Mesophyll Conductance. Implications for the Determination of Rubisco Enzyme Kinetics and for Limitations to Photosynthesis in Vivo. *Plant Physiology*, **130**, 1992-1998

Blackman CJ, Brodribb TJ (2011) Two measures of leaf capacitance: insights into the water transport pathway and hydraulic conductance in leaves. *Functional Plant Biology*, **38**, 118-126

Blackman CJ, Pfautsch S, Choat B, Delzon S, Gleason SM, Duursma RA (2016) Toward an index of desiccation time to tree mortality under drought. *Plant, Cell & Environment*, **39**, 2342-2345

Brodribb TJ, Cochard H (2009) Hydraulic Failure Defines the Recovery and Point of Death in Water-Stressed Conifers. *Plant Physiology*, **149**, 575–584

Brodribb TJ, Holbrook NM (2003) Stomatal Closure during Leaf Dehydration, Correlation with Other Leaf Physiological Traits. *Plant Physiology*, **132**, 2166–2173

Brodribb TJ, McAdam SAM, Carins Murphy MR (2017) Xylem and stomata, coordinated through space and time. *Plant, Cell & Environment*, **40**, 872-880

Brodribb TJ, Skelton RP, McAdam SAM, Bienaimé D, Lucani CJ, Marmottant P (2016) Visual quantification of embolism reveals leaf vulnerability to hydraulic failure. *New Phytologist*, **209**, 1403-1409

Buckley TN (2019) How do stomata respond to water status? *New Phytologist*, **224**, 21-36

Bykova O, Limousin JM, Ourcival JM, Chuine I (2018) Water deficit disrupts male gametophyte development in *Quercus ilex*. *Plant Biology*, **20**, 450-455

Carnicer J, Coll M, Ninyerola M, Pons X, Sanchez G, Peñuelas J (2011) Widespread crown condition decline, food web disruption, and amplified tree mortality with increased climate change-type drought. *PNAS*, **108**, 1474-1478

Charrier G, Delzon S, Domec JC, Zhang L, Delmas CEL, Merlin I, Corso D, King A, Ojeda H, Ollat N, Prieto JA, Scholach T, Skinner P, van Leeuwen C, Gambetta GA (2018) Drought will not leave your glass empty: Low risk of hydraulic failure revealed by long-term drought observations in world's top wine regions. *Science Advances*, **4**, eaao6969

Charrier G, Torres-Ruiz JM, Badel E, Burlett R, Choat B, Cochard H, Delmas CEL, Domec JC, Jansen S, King A, Lenoir N, Martin-StPaul N, Gambetta GA, Delzon S (2016) Evidence for hydraulic vulnerability segmentation and lack of xylem refilling under tension. *Plant Physiology*, **172**, 1657-1668

Cheung YNS, Tyree MT, Dainty J (1975) Water relations parameters on single leaves obtained in a pressure bomb and some ecological interpretations. *Canadian Journal of Botany*, **53**, 1342-1346

Choat B, Brodribb TJ, Brodersen CR, Duursma RA, Lopez R, Medlyn BE (2018) Triggers of tree mortality under drought. *Nature*, **558**, 531-539

Choat B, Jansen S, Brodribb TJ, Cochard H, Delzon S, Bhaskar R, Bucci SJ, Field TS, Gleason SM, Hacke UG, *et al.* (2012) Global convergence in the vulnerability of forests to drought. *Nature*, **491**, 752-755

Cochard H, Badel E, Herbette S, Delzon S, Choat B, Jansen S (2013) Methods for measuring plant vulnerability to cavitation: a critical review. *Journal of Experimental Botany*, **64**, 4779-4791

Cochard H, Coll L, Roux XL, Améglio T (2002) Unraveling the effects of plant hydraulics on stomatal closure during water stress in walnut. *Plant Physiology*, **128**, 282-290

Cochard H, Nardini A, Coll L (2004) Hydraulic architecture of leaf blades: where is the main resistance? *Plant, Cell and Environment*, **27**, 1257-1267

Corcuera L, Cochard H, Gil-Pelegrin E, Notivol E (2011) Phenotypic plasticity in mesic populations of *Pinus pinaster* improves resistance to xylem embolism (P_{50}) under severe drought. *Trees*, **25**, 1033-1042

Creek D, Lamarque LJ, Torres-Ruiz JM, Parise C, Burlett R, Tissue DT, Delzon S (2020) Xylem embolism in leaves does not occur with open stomata: evidence from direct observations using the optical visualization technique. *Journal of Experimental Botany*, **71**, 1151-1159

Davis SD, Mooney HA (1986) Tissue water relations of four co-occurring chaparral shrubs. *Oecologia*, **70**, 527-535

Delzon S, Cochard H (2014) Recent advances in tree hydraulics highlight the ecological significance of the hydraulic safety margin. *New Phytologist*, **203**, 355-358

Dreyer E, Bousquet F, Ducrey M (1990) Use of pressure volume curves in water relation analysis on woody shoots: influence of rehydration and comparison of four European oak species. *Annals of Forest Science*, **47**,285–297

Duursma RA, Blackman CJ, Lopéz R, Martin-StPaul NK, Cochard H, Medlyn BE (2018) On the minimum leaf conductance: its role in models of plant water use, and ecological and environmental controls. *New Phytologist*, **221**, 693-705

Duursma RA, Choat B (2017) fitplc - an {R} package to fit hydraulic vulnerability curves. *Journal of Plant Hydraulics*, **4**, 002

Ewers BE, Oren R (2000) Analyses of assumptions and errors in the calculation of stomatal conductance from sap flux measurements. *Tree Physiology* **20**,579–589

Fichot R, Barigah TS, Chamaillard S, Le Thiec D, Laurans F, Cochard H, Brignolas F (2010) Common trade-offs between xylem resistance to cavitation and other physiological traits do not hold among unrelated *Populus deltoides* x *Populus nigra* hybrids. *Plant, Cell and Environment*, **33**, 1553-1568

Garnier E, Shipley B, Roumet C, Laurent G (2001) A standardized protocol for the determination of specific leaf area and leaf dry matter content. *Functional Ecology*, **15**, 688-695

Gentilesca T, Camarero JJ, Colangelo M, Nolè A, Ripullone F (2017) Drought-induced oak decline in the western Mediterranean region: an overview of current evidences, mechanisms and management options to improve forest resilience. *iForest*, **10**, 796-806

Hacke UG, Stiller V, Sperry JS, Pitterman J, McCulloh KA (2001) Cavitation fatigue. Embolism and refilling cycles can weaken the cavitation resistance of xylem. *Plant Physiology*, **125**, 779-786

Harley PC, Thomas RB, Reynolds JF, Strain BR (1992) Modelling photosynthesis of cotton grown in elevated CO_2. *Plant, Cell and Environment*, **15**, 271-282

Henry C, John GP, Pan R, Bartlett MK, Fletcher LR, Scoffoni C, Sack L (2019) A stomatal safety-efficiency trade-off constrains responses to leaf dehydration. *Nature Communications*, **10**, 3398

Hinckley TM, Duhme F, Hinckley AR, Richter H (1980) Water relations of drought hardy shrubs: osmotic potential and stomatal reactivity. *Plant, Cell and Environment* **3**,131–140

Holloway-Phillips MM, Brodribb TJ (2011) Minimum hydraulic safety leads to maximum water-use efficiency in a forage grass. *Plant, Cell and Environment* **34**, 302–313

Hsiao TC, Acevedo E, Fereres E, Henderson DW (1976) Water stress, growth, and osmotic adjustment. *Philosophical Transactions of the Royal Society B*, **273**, 479-500

Hudson PJ, Limousin JM, Krofcheck DJ, Boutz AL, Pangle RE, Gehres N, McDowell NG, Pockman WT (2018) Impacts of long-term precipitation manipulation on hydraulic architecture and xylem anatomy of piñon and juniper in Southwest USA. *Plant, Cell & Environment*, **41**, 421-435

IPCC – Intergovernmental Panel on Climate Change (2013) Climate Change 2013: The Physical Science Basis. Contribution of Working Group I to the Fifth Assessment Report of the Intergovernmental Panel on Climate Change (eds Stocker TF, Qin D, Plattner G-K,

Tignor M, Allen SK, Boschung J, Nauels A, Xia Y, Bex V, Midgley PM). Cambridge University Press, Cambridge, UK and New York, NY, USA.

Johnson DM, McCulloh KA, Woodruff DR, Meinzer FC (2012) Evidence for xylem embolism as a primary factor in dehydration induced declines in leaf hydraulic conductance. *Plant Cell & Environment*, **35**, 760-769

Jones HG, Sutherland RA (1991) Stomatal control of xylem embolism. *Plant Cell & Environment*, **14**, 607-612

Kim YX, Steudle E (2007) Light and turgor affect the water permeability (aquaporins) of parenchyma cells in the midrib of leaves of *Zea mays*. *Journal of Experimental Botany*, 58, 4119-4129

Klein T (2014) The variability of stomatal sensitivity to leaf water potential across tree species indicates a continuum between isohydric and anisohydric behaviours. *Functional Ecology*, **28**, 1313-1320

Kubiske ME, Abrams MD (1990) Pressure-volume relationships in non-rehydrated tissue at various water deficits. *Plant, Cell and Environment*, **13**, 995–1000

Ladjal M, Huc R, Ducrey M (2005) Drought effects on hydraulic conductivity and xylem vulnerability to embolism in diverse species and provenances of Mediterranean cedars. *Tree Physiology*, **25**, 1109-1117

Lamy JB, Delzon S, Bouche PS, Alia R, Vendramin GG, Cochard H, Plomion C (2014) Limited genetic variability and phenotypic plasticity detected for cavitation resistance in a Mediterranean pine. *New Phytologist*, **201**, 874-886

Lempereur M, Martin-StPaul NK, Damesin C, Joffre R, Ourcival JM, Rocheteau A, Rambal S (2015) Growth duration is a better predictor of stem increment than carbon supply in a Mediterranean oak forest: implications for assessing forest productivity under climate change. *New Phytologist*, **207**, 579-590

Lenz TI, Wright IJ, Westoby M (2006) Interrelations among pressure-volume curve traits across species and water availability gradients. *Physiologia Plantarum*, **127**, 423-433

Le Roncé I, Toïgo M, Dardevet E, Venner S, Limousin JM, Chuine I (2020) Resource manipulation through experimental defoliation has legacy effects on allocation to reproductive and vegetative organs in *Quercus ilex*. *Annals of Botany*, **126**, 1165-1179

Limousin JM, Bickford CP, Dickman LT, Pangle RE, Hudson PJ, Boutz AL, Gehres N, Osuna JL, Pockman WT, McDowell NG (2013) Regulation and acclimation of leaf gas exchange in a piñon-juniper woodland exposed to three different precipitation regimes. *Plant, Cell and Environment*, **36**, 1812-1825

Limousin JM, Longepierre D, Huc R, Rambal S (2010a) Change in hydraulic traits of Mediterranean *Quercus ilex* subjected to long-term throughfall exclusion. *Tree Physiology*, **30**, 1026-1036

Limousin JM, Misson L, Lavoir AV, Martin NK, Rambal S (2010b) Do photosynthetic limitations of evergreen *Quercus ilex* leaves change with long-term increased drought severity? *Plant, Cell and Environment*, **33**, 863-875

Limousin JM, Rambal S, Ourcival, JM, Rocheteau A, Joffre R, Rodriguez-Cortina R (2009) Long-term transpiration change with rainfall decline in a Mediterranean Quercus ilex forest. *Global Change Biology*, **15**, 2163-2175

Lloret F, Siscart D, Dalmases C (2004) Canopy recovery after drought dieback in holm-oak Mediterranean forests of Catalonia (NE Spain). *Global Change Biology*, **10**, 2092-2099

Lobo A, Torres-Ruiz JM, Burlett R, Lemaire C, Parise C, Francioni C, Truffaut L, Tomaskova I, Hansen JK, Kjaer ED, Kremer A, Delzon S (2018) Assessing inter- and intraspecific variability of xylem vunerability to embolism in oaks. *Forest Ecology and Management*, **424**, 53-61

Martinez-Vilalta J, Cochard H, Mencuccini M, Sterck F, Herrero A, Korhonen JFJ, Llorens P, Nikinmaa E, Nolè A, Poyatos R, Ripullone F, Sass-Klaassen U, Zweifel R (2009) Hydraulic adjustment of Scots pine across Europe. *New Phytologist*, **184**, 353-364

Martinez-Vilalta J, Garcia-Forner N (2017) Water potential regulation, stomatal behaviour and hydraulic transport under drought: deconstructing the iso/anisohydric concept. *Plant, Cell & Environment*, **40**, 962-976

Martinez-Vilalta J, Poyatos R, Aguadé D, Retana J, Mencuccini M (2014) A new look at water transport regulation in plants. *New Phytologist*, **204**, 105-115

Martin-StPaul N, Delzon S, Cochard H (2017) Plant resistance to drought depends on timely stomatal closure. *Ecology Letters*, **20**, 1437-1447

Martin-StPaul NK, Limousin JM, Vogt-Schilb H, Rodriguez-Calcerrada J, Rambal S, Longepierre D, Misson L (2013) The temporal response to drought in a Mediterranean evergreen tree: comparing a regional precipitation gradient and a throughfall exclusion experiment. *Global Change Biology*, **19**, 2413-2426

Martin-StPaul N, Ruffault J, Blackmann C, Cochard H, De Caceres M, Delzon S, Dupuy JL, Fargeon H, Lamarque L, Moreno M, Parsell R, Pimont F, Ourcival JM, Torres-Ruiz J, Limousin JM (2020) Modelling live fuel moisture content at leaf and canopy scale under extreme drought using a lumped plant hydraulic model. *BioArxiv*, https://www.biorxiv.org/content/10.1101/2020.06.03.127167v1

Martorell S, Medrano H, Tomas M, Escalona JM, Flexas J, Diaz-Espejo A (2015) Plasticity of vulnerability to leaf hydraulic dysfunction during acclimation to drought in grapevines: an osmotic-mediated process. *Physiologia Plantarum*, **153**, 381-391

McDowell N, Pockman WT, Allen CD, Breashears DD, Cobb N, Kolb T, Plaut J, Sperry J, West A, Williams DG, Yepez EA (2008) Mechanisms of plant survival and mortality during drought: why do some plants survive while others succumb to drought? *New Phytologist*, **178**, 719-739

Meinzer FC, Woodruff DR, Marias DE, McCulloh KA, Sevanto S (2014) Dynamics of leaf water relations components in co-occuring iso- and anisohydric conifer species. *Plant, Cell and Environment*, **37**, 2577-2586

Meinzer FC, Woodruff DR, Marias DE, Smith DD, McCulloh KA, Howard AR, Magedman AL (2016) Mapping 'hydroscapes' along the iso- to anisohydric continuum of stomatal regulation of plant wáter status. *Ecology Letters*, **19**, 1343-1352

Mencuccini M, Grace J (1995) Climate influences on the leaf area / sapwood area ratio in Scots pine. *Tree Physiology*, **15**, 1-10

Moreno M, Simioni G, Cailleret M, Ruffault J, Badel E, Carrière S, Davi H, Gavinet J, Huc R, Limousin JM, Marloie O, Martin L, Rodriguez-Calcerrada J, Vennetier M, Martin-StPaul N (2021) Consistently lower sap velocity and growth over nine years of rainfall exclusion in a Mediterranean mixed pine-oak forest. *Agricultural and Forest Meteorology*, **308-309**, 108472

Morgan JM (1984) Osmoregulation and water stress in higher plants. *Annual Review of Plant Physiology*, **35**, 299-319

Nardini A, Luglio J (2014) Leaf hydraulic capacity and drought vulnerability: posible trade-offs and correlations with climate across three major biomes. *Functional Ecology*, **28**, 810-818

Nardini A, Pedà G, La Rocca N (2012) Trade-offs between leaf hydraulic capacity and drought vulnerability: morpho-anatomical bases, carbon costs and ecological consequences. *New Phytologist*, **196**, 788-798

Niinemets U, Cescatti A, Rodeghiero M, Tosens T (2005) Leaf internal diffusion limits photosynthesis more strongly in older leaves of Mediterranean evergreen broad-leaved species. *Plant, Cell and Environment*, **28**, 1552-1566

Nolan RH, Tarin T, Santini NS, McAdam SAM, Ruman R, Eamus D (2017) Differences in osmotic adjustment, foliar abscisic acid dynamics, and stomatal regulation between isohydric and anisohydric woody angiosperm during drought. *Plant, Cell and Environment*, **40**, 3122-3134

Rodriguez-Calcerrada J, Jaeger C, Limousin JM, Ourcival JM, Joffre R, Rambal S (2011) Leaf CO_2 efflux is attenuated by acclimation of respiration to heat and drought in a Mediterranean tree. *Functional Ecology*, **25**, 983-995

Rodríguez-Calcerrada J, Sancho-Knapik D, Martin-StPaul NK, Limousin JM, McDowell NG, Gil-Pelegrín E (2017) Drought-induced oak decline – factors involved, physiological dysfunctions, and potential attenuation by forestry practices. In Gil-Pelegrín *et al.* (eds) Oaks physiological ecology. Exploring the functional diversity of genus *Quercus* L. Springer International Publishing, Tree Physiology **7**: 419-451

Rodriguez-Dominguez CM, Buckley TN, Egea G, de Cires A, Hernandez-Santana V, Martorell S, Diaz-Espejo A (2016) Most stomatal closure in woody species under moderate drought can be explained by stomatal responses to leaf turgor. *Plant, Cell and Environment*, **39**, 2014-2026

Sack L, Cowan PD, Jaikumar N, Holbrook NM (2003) The 'hydrology' of leaves: co-ordination of structure and function in temperate woody species. *Plant, Cell and Environment*, **26**, 1343-1356

Salleo S, Lo Gullo MA (1990) Sclerophylly and plant water relations in three Mediterranean *Quercus* species. *Annals of Botany*, **65**, 259-270

Salleo S, Nardini A, Pitt F, Lo Gullo MA (2000) Xylem cavitation and hydraulic control of stomatal conductance in Laurel (*Laurus nobilis* L.). *Plant, Cell & Environment*, **23**, 71-79

Salmon Y, Torres-Ruiz JM, Poyatos R, Martinez-Vilalta J, Meir P, Cochard H, Mencuccini M (2015) Balancing the risk of hydraulic failure and carbon starvation: a twig scale analysis in declining Scots pine. *Plant, Cell and Environment*, **38**, 2575-2588

Salomon RL, Limousin JM, Ourcival JM, Rodríguez-Calcerrada J, Steppe K (2017) Stem hydraulic capacitance decreases with drought stress: implications for modelling tree hydraulics in the Mediterranean oak *Quercus ilex*. *Plant, Cell and Environment*, **40**, 1379-1391

Salomon RL, Steppe K, Ourcival JM, Villers S, Rodríguez-Calcerrada J, Schapman R, Limousin JM (2020) Hydraulic acclimation in a Mediterranean oak subjected to permanent throughfall exclusion results in increased stem hydraulic capacitance. *Plant, Cell and Environment*, **43**, 1528-1544

Schuldt B, Knutzen F, Delzon S, Jansen S, Müller-Haubold H, Burlett R, Clough Y, Leuschner C (2016) How adaptable is the hydraulic system of European beech in the face of climate change-related precipitation reduction? *New Phytologist*, **210**, 443-458

Scoffoni C, Albuquerque C, Brodersen CR, Townes ST, John GP, Bartlett MK, Buckley TN, McElrone AJ, Sack L (2017) Outside-xylem tissue vulnerability, not xylem embolism, controls leaf hydraulic decline with dehydration across diverse angiosperms. *Plant Physiology*, **173**, 1197-1210

Scoffoni C, McKown AD, Rawls M, Sack L (2011) Dynamics of leaf hydraulic conductance with water status: quantification and analysis of species differences under steady-state. *Journal of Experimental Botany*, **63**, 643-658

Scoffoni C, Sack L (2017) The causes and consequences of leaf hydraulic decline with dehydration. *Journal of Experimental Botany*, **68**, 4479-4496

Scoffoni C, Vuong C, Diep S, Cochard H, Sack L (2014) Leaf Shrinkage with Dehydration: Coordination with Hydraulic Vulnerability and Drought Tolerance. *Plant Physiology*, **164**, 1772-1788

Senf C, Buras A, Zang CS, Rammig A, Seidl R (2020) Excess forest mortality is consistently linked to drought across Europe. *Nature Communications*, **11**, 6200

Sergent AS, Varela SA, Barigah TS, Badel E, Cochard H, Dalla-Salda G, Delzon S, Fernandez ME, Guillemot J, Gyenge J, Lamarque LJ, Martinez-Meier A, Rozenberg P, Torres-Ruiz JS, Martin-StPaul NK (2020) A comparison of methods to assess embolism resistance in trees. *Forest Ecology and Management*, **468**, 118175

Shatil-Cohen A, Attia Z, Moshelion M (2011) Bundle-sheath cell regulation of xylem-mesophyll water transport via aquaporins under drought stress: a target of xylem-borne ABA? *The Plant Journal*, **67**, 72-80

Sorek Y, Greenstein S, Netzer Y, Shtein I, Jansen S, Hochberg U (2020) An increase in xylem embolism resistance of grapevine leaves during the growing season is coordinated with stomatal regulation, turgor loss point and intervessel pit membranes. *New Phytologist*, **229**, 1955-1969

Sperry JS (2000) Hydraulic constraints on plant gas exchange. *Agricultural and Forest Meteorology*, **104**, 13-23

Sperry JS, Wang Y, Wolfe BT, Mackay DS, Anderegg WRL, McDowell NG, Pockman WT (2016) Pragmatic hydraulic theory predicts stomatal responses to climatic water deficits. *New Phytologist*, **212**, 577-589

Thomas FM, Gausling T (2000) Morphological and physiological responses of oak seedlings (*Quercus petraea* and *Q. robur*) to moderate drought. *Annals of Forest Sciences*, **57**, 325-333

Torres-Ruiz JM, Diaz-Espejo A, Perez-Martin A, Hernandez-Santana V (2015) Role of hydraulic and chemical signals in leaves, stems and roots in the stomatal behavior of olive trees under water stress and recovery conditions. *Tree Physiology*, **35**, 415-424

Torres-Ruiz JM, Kremer A, Carins-Murphy MR, Brodribb TJ, Lamarque LJ, Truffaut L, Bonne F, Ducousso A, Delzon S (2019) Genetic differentiation in functional traits among European sessile oak populations. *Tree Physiology*, **39**, 1736-1749

Tramblay Y, Koutroulis A, Samaniego L, Vicente-Serrano SM, Volaire F, Boone A, Le Page M, Llasat MC, Albergel C, Burak S, Cailleret M, Kalin KC, Davi H, Dupuy JL, Greve P,

Grillakis M, Haniche L, Jarlan L, Martin-StPaul N, Martinez-Vilalta J, Mouillot F, Pulido-Velazquez D, Quintana-Segui P, Renard D, Turco M, Turkes M, Trigo R, Vidal JP, Vilagrosa A, Zribi M, Polcher J (2020) Challenges for drought assessment in the Mediterranean region under future climate scenarios. *Earth-Science Reviews*, **210**, 103348

Trenberth KE, Dai A, van der Schrier G, Jones PD, Barichivich J, Briffa KR, Sheffield J (2014) Global warming and changes in drought. *Nature Climate Change*, **4**, 17-22

Trifilo P, Raimondo F, Savi T, Lo Gullo MA, Nardini A (2016) The contribution of vascular and extra-vascular water pathways to drought-induced decline of leaf hydraulic conductance. *Journal of Experimental Botany*, **67**, 5029-5039

Trueba S, Pan R, Scoffoni C, John GP, Davis SD, Sack L (2019) Thresholds for leaf damage due to dehydration: declines of hydraulic function, stomatal conductance and cellular integrity precede those for photochemistry. *New Phytologist*, **223**, 134-149

Tyree MT, Cochard H, Cruziat P, Sinclair B, Ameglio T (1993) Drought-induced leaf shedding in walnut: evidence for vulnerability segmentation. *Plant, Cell & Environment*, **16**, 879-882

Tyree MT, Ewers FW (1991) The hydraulic architecture of trees and other woody-plants. *New Phytologist*, **119**, 345-360

Tyree MT, Sperry JS (1988) Do woody plants operate near the point of catastrophic xylem dysfunction caused by dynamic water stress? Answers from a model. *Plant Physiology*, **88**, 574-580

Wolfe BT, Sperry JS, Kursar TA (2016) Does leaf shedding protect stems from cavitation during seasonal droughts? A test of the hydraulic fuse hypothesis. *New Phytologist*, **212**, 1007-1018

Wortemann R, Herbette S, Barigah TS, Fumanal B, Alia R, Ducousso A, Gomory D, Roeckel-Drevet P, Cochard H (2011) Genotypic variability and phenotypic plasticity of cavitation resistance in *Fagus sylvatica* L. across Europe. *Tree Physiology*, **31**, 1175-1182

Zhu SD, Liu H, Xu QY, Cao KF, Ye Q (2016) Are leaves more vulnerable to cavitation than branches? *Functional Ecology*, **30**, 1740-1744